Electrocatalytic Oxygen Evolution Reaction in Acidic Environments – Reaction Mechanisms and Catalysts

Tobias Reier[1], Hong Nhan Nong[1], Detre Teschner[2], Robert Schlögl[2] and Peter Strasser[1,3]*

[1] *The Electrochemical Energy, Catalysis and Materials Science Laboratory, Department of Chemistry, Chemical Engineering Division, Technical University Berlin, Strasse des 17. Juni 124, 10623 Berlin, Germany*

[2] *Department of Inorganic Chemistry, Fritz-Haber-Institute of the Max-Planck-Society, Faradayweg 4-6, 14195 Berlin, Germany*

[3]*Ertl Center for Electrochemistry and Catalysis, Gwangju Institute of Science and Technology, Gwangju 500-712, South Korea*

Abstract

The low efficiency of the electrocatalytic oxidation of water to O_2 (oxygen evolution reaction-OER) is considered as one of the major roadblocks for the storage of electricity from renewable sources in form of molecular fuels like H_2 or hydrocarbons. Especially in acidic environments, compatible with the powerful proton exchange membrane (PEM), an earth-abundant OER catalyst that combines high activity and high stability is still unknown. Current PEM-compatible OER catalysts still rely mostly on Ir and/or Ru as active components, which are both very scarce elements of the platinum group. Hence, their amount in OER catalysts has to be strictly minimized in order to facilitate the economically competitive large-scale application of PEM electrolyzers. Unfortunately, the OER mechanism, which is the most powerful tool for catalyst optimization, still remains unclear. In this review, we first review the current state of our understanding of the OER mechanism of PEM-compatible heterogeneous electrocatalysts, before we compare and contrast that to the OER mechanism on homogenous catalysts. Thereafter, an overview over monometallic OER catalysts is provided followed by a review of current material optimization concepts. Moreover, missing links required to complete the mechanistic picture as well as the most promising material optimization concepts are pointed out.

1. Introduction

Renewable electricity generation technologies, like wind and solar power, are promising candidates to achieve a clean and sustainable energy infrastructure. However, wind and solar power are both characterized by an intermittent availability.[1] Thus, a large scale energy storage solution is required in order to bridge the time gap between supply and demand. Molecular fuels like hydrogen or hydrocarbons produced from renewable electricity and water or, respectively, CO_2 can provide such a long term chemical energy storage solution.[1, 2, 3] Considering hydrogen, its reconversion to electrical energy can be efficiently performed in fuel cells.[4] In a transition period, hydrogen can additionally be used as fuel for combustion engines, which underlines its versatility. Besides that, hydrogen and hydrocarbons can be appropriately used for mobile applications due to their comparably high gravimetric energy density.[2] The electrocatalytic production of molecular fuels like hydrogen from water or hydrocarbons from CO_2 is based on reduction reactions which, in turn, require an electron donating counter reaction. In this context, the electrocatalytic oxidation of water to molecular oxygen, the oxygen evolution reaction (OER), is the most promising candidate with regard to availability and sustainability.[5] Additionally, the OER constitutes a common counter reaction in metal electrowinning.[6] Hence, the OER is not only a key step for electricity storage but is furthermore of outmost importance in other processes. Unfortunately, the OER is a complex multistep reaction, which adds a considerably large overpotential to the actual process and, thus, distinctly reduces the process efficiency even if current benchmark catalysts are applied.[5] Additionally, the inherent high electrode potentials during the OER are demanding with respect to the catalysts stability.

In the context of water electrolysis for renewable electricity storage, proton exchange membrane (PEM) electrolyzers offer great advantages compared to alkaline electrolyzers such as lower ohmic losses, higher voltage efficiency, higher gas purity, a more compact system design, higher current density, a faster system response and a larger partial load range.[7, 8] The aforementioned advantages are directly or indirectly related to the PEM, which is an acidic solid polymer electrolyte membrane. In particular, the PEM ensures a small gas crossover and provides a high proton conductivity.[7] Since the gas crossover is rather independent of the applied load, gas crossover becomes problematic at low loads where gas production rates are low.[7] In this case, the transport rate of H_2 through the membrane can be high enough to form H_2-O_2 mixtures that approach or exceed the explosion limit, which has to be strictly avoided for safety reasons.[9] Therefore, electrolyzers can only be operated above a certain load. Comparing PEM and alkaline electrolyzers, this minimal load is commonly much smaller for PEM electrolyzers, due to the comparably small gas crossover of PEMs. [7, 9] Based on the large load range and the fast system response, PEM electrolyzers offer a great flexibility to respond to the intermittent electricity generation from renewable sources. Furthermore, the high proton conductivity of PEMs ensures low ohmic losses and the applicability of high current densities,[7] which are not only advantageous in the context of renewable electricity storage. In contrast to the well-established

fully-developed PEMs, alkaline solid polymer electrolytes are currently under development but commercial alkaline electrolyzers still rely on liquid electrolytes in combination with diaphragms.[7, 10] Furthermore, all alkaline electrolytes have the intrinsic drawback that the equivalent conductivity of hydroxide ions (198 S cm^2 mol^{-1})[11] is considerably lower than that of hydronium ions (350 S cm^2 mol^{-1})[11]. Thus, acidic electrolytes (membranes) potentially provide (at similar thickness and charge carrier concentration) much lower ohmic resistances, which is especially relevant to minimize losses at high current densities on the application level.

Besides the aforementioned disadvantages of alkaline electrolyzers, their major advantage is the comparably wide range of abundant materials that are applicable as anode catalysts, such as Fe, Ni, Co, Cu and Mn based oxides as well as nitrogen doped carbon materials.[12, 13] However, while OER catalysis profits from alkaline conditions, the cathode reaction, the hydrogen evolution reaction (HER), is usually impeded in an alkaline environment.[14] This circumstance lowers the possible gain on the system level. In contrast to alkaline electrolyzers, one main shortcoming of PEM electrolyzers is the limited range of materials for the anode catalyst and related parts such as current collectors and separator plates[7], since these materials must sustain high electrode potentials in combination with the acidic environment. The vast majority of PEM compatible anode catalysts is based on oxides of Ru and, especially, Ir which are, unfortunately, very scarce noble metals[7] with annual production capacities far below that of Pt[15]. Hence, pricing and availability of Ru and Ir can be considered as a major issue for the large-scale application of PEM electrolyzers. Thus, in order to profit from the numerous advantages of PEM electrolyzers and facilitate their large-scale application, the noble metal amount required in the anode catalyst need to be drastically reduced. For this purpose, an in-depth fundamental understanding of the OER mechanism and the applied catalyst materials in acidic environment is required. Based on this knowledge, new strategies for catalyst design and optimization can be established to minimize the noble metal content while preserving a high activity and stability for the OER.

In this review, first the different OER mechanisms proposed in acidic environment are reviewed. As a next step, the present status of the experimentally determined OER mechanism of homogenous Ru catalysts is summarized to provide the basis for the subsequent discussion of in-situ analytical insights from heterogeneous OER catalysts. Then, to provide insights into structure-function relations of PEM compatible OER catalysts, activity and stability trends of monometallic OER catalysts are reviewed. Based on this knowledge, new catalyst optimization approaches are discussed to point out their potential for future research.

2. The oxygen evolution reaction mechanism in acidic environment- Current state of knowledge

2.1. Heterogeneous catalysts

To date, a number of different reaction mechanisms have been proposed for the OER on heterogeneous electro-catalysts, based on kinetic studies[16, 17, 18] or theoretical density functional theory (DFT) based calculations[19-22], some of which are shown in Figure 1. However, none of the reaction mechanisms proposed for heterogeneous catalysts has been yet fully validated based on experimental results. In a pioneering work, Bockris made up kinetic models for a variety of different conceivable OER mechanisms, some of which are shown in Figure 1 I-III.[16] Bockris demonstrated that the Tafel slope, observable in an electrocatalytic measurement, is determined by the actual rate determining step (rds) within a certain reaction mechanism.[16] This analysis was based on the assumption that one step in each reaction mechanism is the rds and that only the reactant of the rds can build up a considerably high surface coverage (concentration).[16] Considering RuO_2, the Tafel slope analysis revealed a reaction mechanism similar to the *electrochemical oxide path* (see Figure 1 II) with an additional chemical rearrangement step of the M-OH species between reaction 1 and 2.[18, 23] Below 1.52 V this rearrangement step was found to be rate determining whereas at higher potentials the first step (step 1 in Figure 1 II) becomes rate determining.[18, 23] However, a rds cannot unambiguously be identified based on the Tafel slope alone. Different rds in different mechanisms can result in similar Tafel slopes.[16] Furthermore, the actual reaction mechanism might not have been considered in the set of mechanism for which the Tafel slopes have been deduced. Moreover, the Tafel slope itself is a somewhat unspecific measure which can be altered by factors besides the electrocatalytic reaction. Scheuermann et al. have for instance shown that a semiconducting oxide layer, located between catalyst and substrate (current collector), can increase the Tafel slope.[24] Thus, precise knowledge about the electrodes material properties, especially with respect to conductivity and possible buried interfaces, is required in order to obtain valid mechanistic insights from a Tafel slope analysis.

I)	Oxide Path	II)	Electrochemical Oxide Path
1)	$H_2O + M \rightarrow M\text{-}OH + H^+ + e^-$	1)	$H_2O + M \rightarrow M\text{-}OH + H^+ + e^-$
2)	$2\,M\text{-}OH \rightarrow M\text{-}O + M + H_2O$	2)	$M\text{-}OH \rightarrow M\text{-}O + H^+ + e^-$
3)	$2\,M\text{-}O \rightarrow 2\,M + O_2$	3)	$2\,M\text{-}O \rightarrow 2\,M + O_2$
III)	**Electrochemical Metal Peroxide Path**	**IV)**	**DFT-predicted Peroxide Path**
1)	$H_2O + M \rightarrow M\text{-}OH + H^+ + e^-$	1)	$H_2O + M \rightarrow M\text{-}OH + H^+ + e^-$
2)	$2\,M\text{-}OH \rightarrow M\text{-}O + M + H_2O$	2)	$M\text{-}OH \rightarrow M\text{-}O + H^+ + e^-$
3)	$M\text{-}O + H_2O \rightarrow M\text{-}OOH + H^+ + e^-$	3)	$M\text{-}O + H_2O \rightarrow M\text{-}OOH + H^+ + e^-$
4)	$2\,M\text{-}OOH \rightarrow M\text{-}O + H_2O + O_2 + M$	4)	$M\text{-}OOH \rightarrow M + O_2 + H^+ + e^-$

Figure 1: Proposed reaction mechanisms for the oxygen evolution reaction. Reaction

mechanisms I-III were taken (adapted) from reference [16] whereas reaction mechanism IV was obtained from reference [22].

Another concept based on which an OER mechanism has been proposed is the thermochemical analysis using DFT calculations, as demonstrated by Rossmeisl et al.[20-22] Here, first a mechanism is proposed (see Figure 1 IV). Then, the Gibbs free energy of every reaction ($\Delta_R G_x$) within the mechanism is calculated as a function of the electrode potential. In this context, only elementary reactions in which an electron is exchanged with the electrode are considered, since only these steps depend directly on the electrode potential. To facilitate the overall reaction, as a necessary condition, $\Delta_R G_x$ of every reaction step has to be ≤ 0 J mol^{-1} (compare Figure 2). Although the sum of $\Delta_R G_x$ of the individual reaction steps has to equal $\Delta_R G$ of the overall reaction (oxidation from water to O_2), each reaction step can have a different $\Delta_R G_x$ within the mentioned boundary condition. If one electron is transferred to the catalyst in each step, $\Delta_R G_x$ of each step changes equally with electrode potential. The reaction step which displays the largest $\Delta_R G_x$ (at the reference potential of 0 V_{SHE}) requires the highest electrode potential to be become downhill in $\Delta_R G$ (step 3 in Figure 2 requires 1.60 V) and, thus, is referred to as the potential determining step (pds).[25] Hence, there can be reaction steps that require a higher electrode potential than the standard potential of the overall reaction (E_0=1.23 V) to meet the condition of $\Delta_R G_x \leq 0$ J mol^{-1}, see Figure 2. In contrast to the overall reaction, $\Delta_R G_x$ of the reaction steps (see Figure 1 IV and Figure 2) depends on the adsorption energy of the intermediates and, thus, is a function of the catalyst. Hence, the potential required to facilitate the overall reaction is a function of the catalyst. Since this approach describes the reactivity trend on different catalysts fairly good, the validity of the proposed mechanism appears reasonable, although the model is based on thermodynamics alone and does not account for any kinetic barrier. This treatment, however, does not mean that there are no kinetic barriers but it assumes that the kinetic barriers scale with the thermodynamic barriers and, thus, the reactivity trend can be qualitatively explained on a thermodynamic basis. Additionally, reaction mechanism IV includes the implicit assumption that proton and electron transfer are coupled in every step. Indeed, Nakagawa et al. found that the OER overpotential on a heterogeneous Ir oxide catalyst does not depend on the pH value, which supports the assumption of a coupled proton-electron transfer.[26, 27] However, the occurrence of a coupled or, rather, a sequential proton electron transfer can depend on the interaction strength between catalyst and intermediates and, hence, might be a function of the actual catalyst.[27]

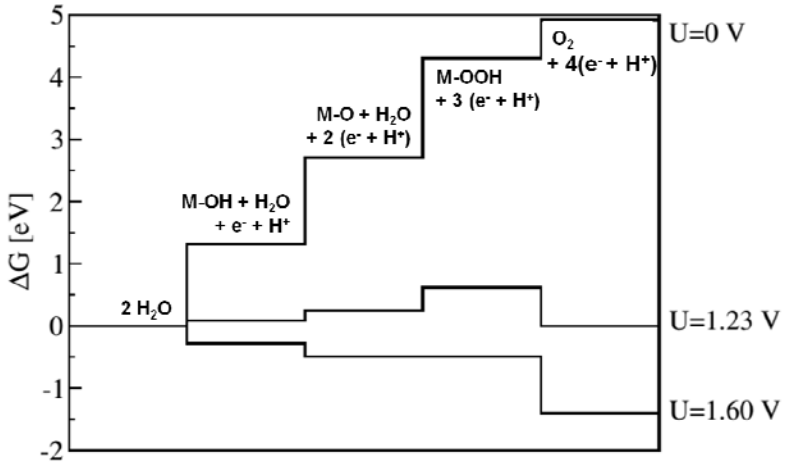

Figure 2: Gibbs free energies of assumed reaction intermediates of the oxygen evolution reaction (OER) on a (1 1 0) RuO_2 surface covered with O. The Gibbs free energies are depicted for three different electrode potentials: 0 V, 1.23 V (equilibrium potential of the overall reaction) and 1.60 V vs. standard hydrogen electrode (SHE). At 1.60 V vs. SHE the OER becomes thermodynamically feasible ($\Delta_R G \leq 0$ eV under the considered conditions). Reprinted (adapted) with permission from reference [22].[28]

In order to minimize the potential which is required to trigger the reaction thermodynamically on a given catalyst, $\Delta_R G_x$ of the reactions in mechanism (IV) (Figure 1) has to be optimized by tuning the binding energy of the M-OH, M-O and M-OOH intermediates. As demonstrated by Rossmeisl et al., these binding energies are linearly correlated and, hence, they cannot be varied independently.[21, 22] This restricts the optimization of the catalyst so that the thermodynamic potential of the overall reaction cannot be reached.[20, 22] However, recently Halck et al. have shown that the correlation of the binding energies can be overcome by doping the oxides surface with a second metal like Co or Ni.[19] Commonly, the coordinatively unsaturated sites (cus, metal surface atoms in an oxide that have a smaller coordination number compared to the bulk (see Figure 3)) are expected to constitute the active center for the OER.[19, 20, 22] However, it was found that a dopant like Co or Ni lowers the OER overpotential of RuO_2, if it is located in the bridge site.[19] If the dopant is present in the bridge site, it is expected to activate the oxygen atom above as proton donor-acceptor functionality (see Figure 3). This proton donor-acceptor functionality can be used to transfer hydrogen away from M-OH or M-OOH reaction intermediates resulting in a lowering of their energetic state.[19] With this additional parameter, which primarily affects two of three OER intermediates, the linear correlation of the binding energies (scaling relations) can be overcome.[19] Thus, this theoretical model points out a possible way for the design of highly active OER catalysts. However, a more detailed theoretical study by Fang et al. for the OER on RuO_2(110) revealed that the bridging O acts even on pure RuO_2 as a proton acceptor functionality, which is critically important for the reactivity.[29] Similar to the reaction mechanism

introduced by Rossmeisl et al. (Figure 1 IV), Fang et al. found that an attack of water in the O-O bond formation step is preferred over a coupling of two surface O groups.[29] Since the calculated results are in good agreement with experimental OER results on RuO_2, the model appears to represent the actual reaction mechanism.[23, 29] Chen et al. demonstrated in a theoretical study that the electronic properties of bridging O sites on RuO_2, which act as proton acceptor, are highly relevant for the OER activity and can be altered by doping with other metal cations such as Ni, Co or Ir.[30]

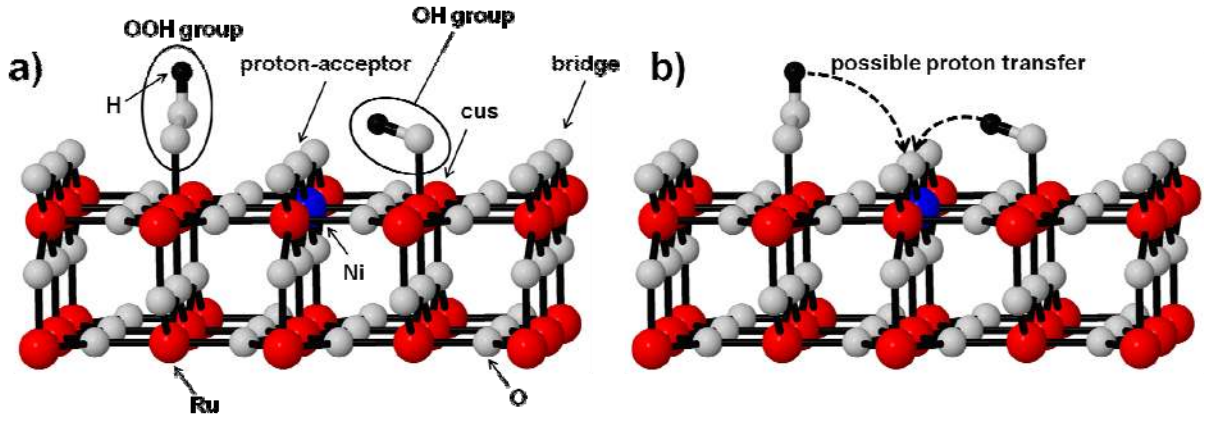

Figure 3: Schematic representation of (1 1 0) surface of a rutile type oxide like RuO_2. The coordinatively unsaturated (cus) as well as the bridge sites are labeled. One ion in a bridge site is exchanged by a lower valent Ni ion. An OH and an OOH group are adsorbed on a cus site, respectively. In a) the different surface species are labeled. In b) possible proton transfer is exemplified, as the bridging O related to Ni are activated as proton donor-acceptor functionality.[19] Bond angles and length of adsorbed intermediates are provided as schematic representation and do not represent the actual state during the reaction.

As was shown above, the thermo-chemical analysis is a very useful tool to describe trends in OER catalysis and, hence, helps to identify possible new materials and material combinations. However, the thermochemical analysis is not necessarily able to unravel the precise nature of the reaction mechanism, because it does not include kinetic barriers.[31] As pointed out by Mavros et al., two different OER mechanisms calculated based on a thermo-chemical approach yielded the same overpotentials within the experimental uncertainty.[31] This outcome underlines the need for more sophisticated calculations and in-situ studies to unambiguously clarify the actual OER mechanism.

In contrast to heterogeneous catalysts, a more detailed understanding of the OER mechanism has already been established for homogeneous catalysts. Most homogenous OER catalysts are well suited for in-situ studies for instance by resonance Raman spectroscopy, EPR, XANES as well as EXAFS, which allowed to establish rather deep mechanistic insights that are not available for heterogeneous OER catalysts. The absence of a ‘spectator’ bulk phase makes the detection of

OER-related changes and intermediates in homogenous OER catalysts more straightforward. Moreover, a defined coordination environment together with the possibility of its variation in homogenous OER catalysts allows for the evaluation of the significance of certain groups and geometries around the active metal center. In contrast to that, polycrystalline materials with their ill-defined surface structure are often used for in-situ studies of heterogeneous catalysts. Even if single crystals are applied, the variation of the coordination environment of surface atoms is not straightforward. However, as recently pointed out by Exner et al., ligand effects are also of potential interest for heterogeneous OER catalysts in order to tune the metal-oxygen bond strength to the optimum.[32]

Two fundamentally different OER mechanisms, the *acid-base* and *the direct coupling mechanism*, which differ primarily with respect to their O-O bond formation step (see Figure 4a), are conceivable for heterogeneous and homogenous catalysts.[31] In terms of heterogeneous catalysis, the *acid-base mechanism* corresponds to an *Eley-Rideal* like mechanism whereas the *direct coupling mechanism* corresponds to a *Langmuir-Hinshelwood* like mechanism. Both start from adsorbed M-OH species which are then transferred into M-O species by oxidation of the metal site to which they are coordinated.[31] Then, within the so called *direct coupling mechanism*, two neighboring M-O species couple directly to form an O-O bond whereas in the so called *acid-base mechanism* the M-O species undergoes a nucleophilic attack of water resulting in an M-OOH species (see Figure 4a).[31] Within the direct coupling mechanism, the O-O bond formation can also proceed between an M-O and an M-OH species resulting in an M-OOH intermediate.[33] The M-OOH species is further oxidized to an M-OO species which is then, in the next step, replaced by water while O_2 is released. Evidence for the *direct coupling mechanism* was reported for the CoCat.[33, 34] In contrast to that, the *acid-base mechanism* is commonly considered for homogenous Ru based OER catalysts[35, 36, 37]. One powerful approach to differentiate between these mechanisms is to perform the reaction with isotope-labeled catalysts or reactants. If for instance the M-OH species in the catalyst are labeled as ^{18}OH and the reaction is performed in $H_2{}^{16}O$, then if $^{18}O^{18}O$ could be found in the product by mass spectroscopy in the early stages of the reaction, it would be a clear indication for the *direct coupling mechanism*.

2.2. Homogeneous catalysts

Based on homogenous complex catalysts, it was shown that the OER can be performed at a single metal site such as Ru, Ir, Fe, Co or Mn.[38] In case of homogeneous mononuclear Ru complexes, the ligands have a strong impact on the catalytic OER performance.[38] Based on the well-studied $[Ru^{II}(bpy)(tpy)H_2O]^{2+}$ (bpy: 2,2'-bipyridine, tpy: 2,2':6',2''-terpyridine, see Figure 4b), in which substituents were introduced on the bpy and/or the tpy ligand, it was shown as a general trend that electron donating substituents improve the catalytic activity.[39] For $[Ru^{II}(bpy)(tpy)H_2O]^{2+}$ the reaction mechanism depicted in Figure 4b was proposed.[40] Therein, Ru is first oxidized from (II) to (IV) (state 1 to 3). Hereby, the deprotonation of the water ligand avoids the formation of highly charged energetically unfavorable intermediates. In strongly acidic media, two protons are

released from state 2 to 3 while no proton transfer occurs from state 1 to 2.[38] In contrast to that, at higher pH values one proton is transferred in each step.[38] If in $[Ru^{II}(bpy)(tpy)H_2O]^{2+}$ the water ligand is substituted by a chloride ligand, Ru cannot be oxidized above Ru(III), since the charge cannot be balanced by proton transfer.[40] The importance of proton transfer for the homogenously catalyzed OER was supported by the facts that a kinetic isotope effect was observed upon H_2O/D_2O exchange (catalyst: [Ru(tpy)(3-methyl-1-pyridylbenzimidazol-2-ylidene)$(OH_2)]^{2+}$)[41] and that the addition of a base increased the OER rate (catalyst: [Ru(2,6-bis(1-methylbenzimidazol-2-yl)pyridine))(bpy)$(OH_2)]^{2+}$).[38, 42] As shown recently, state (3) with Ru (IV) represents the majority species during the catalytic OER cycle of $[Ru^{II}(bpy)(tpy)H_2O]^{2+}$.[40] In the next step, Ru was postulated to be further oxidized to an Ru(V)=O species, (3.1) without a coupled proton transfer, which then undergoes a nucleophilic attack by water.[35] However, there is some uncertainty over the existence of such a Ru(V) species, because it could not be detected by EPR spectroscopy.[40] Therefore, an additional pathway was proposed in which the attack of water as well as the oxidation of the complex appear concerted and, thus, the reaction proceeds directly from (3) to (4).[40] In contrast to that, there is clear evidence for at least one Ru(V) species in case of the so called blue dimer (*cis,cis*-$[(bpy)_2(H_2O)Ru^{III}ORu^{III}(OH_2)(bpy)_2]^{4+}$, see Figure 5), a well-known binuclear Ruthenium water oxidation catalyst.[37, 43] However, as product of the nucleophilic attack of water, a complex with an OOH species (4) is the product, which again is oxidized in a coupled proton-electron transfer ((4) to (5)).[40] In the last step, the O-O species in (5) is substituted by a water molecule whereby molecular oxygen is released and the catalytic cycle is closed. It appears also possible that Ru is oxidized to Ru(V) before O_2 is released as represented by intermediate (5.1).[40] In conclusion, even in case of homogenous catalysts some controversy exists about the oxidation state during the O-O bond formation step.

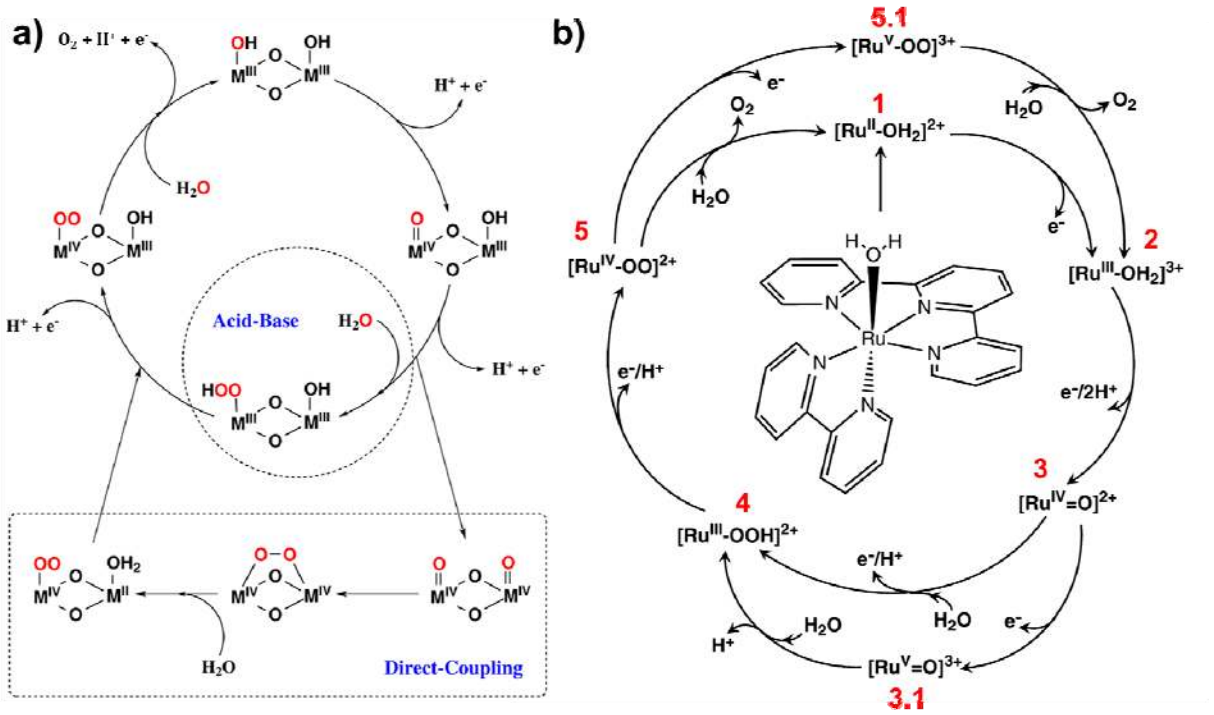

Figure 4: a) Illustration of the Acid-Base and Direct-Coupling OER mechanism classified according to the O-O bond formation step. Reprinted (adapted) with permission from reference [31]. Copyright (2014) American Chemical Society. b) Detailed reaction mechanism proposed for the oxygen evolution reaction on $[Ru^{II}(bpy)(tpy)H_2O]^{2+}$ *as homogeneous catalyst (acid-base type). All intermediates of the reaction are numbered to be easily referable within the text. Reprinted (adapted) with permission from reference [40]. Copyright (2014) American Chemical Society.*

Even if a binuclear Ru complex such as the well-studied blue dimer (see Figure 5) is considered, the OER was not observed to proceed via a direct coupling of vicinal oxygen species.[37] Although it was shown that one Ru center alone is able to catalyze the OER, a second neighboring Ru site, connected via a μ-oxo bridge, is beneficial for the OER performance inter alia by stabilizing higher Ru oxidation states and giving the possibility of hydrogen bond formation with intermediates of the water oxidation process.[44] The μ-oxo bridge itself in the blue dimer is not oxidized to molecular oxygen during the OER.[37] Thereby, the μ-oxo bridge shows some similarities to the bridging O on rutile type (110) surfaces, since it acts as proton acceptor within the mechanism but is not oxidized to O_2[19, 29].

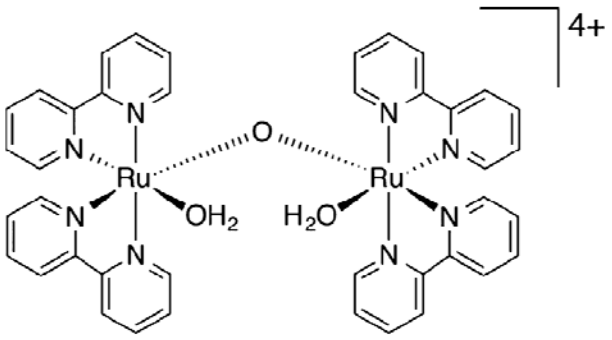

Figure 5: Binuclear homogenous oxygen evolution catalyst (blue dimer). Reprinted with permission from reference [31]. Copyright (2014) American Chemical Society.

3. In-situ insights into the OER mechanism

At this point the question remains, as to which extent the knowledge obtained from homogeneous catalysts is transferrable to heterogeneous catalysts. As pointed out by Crabtree, the boundary between both fields is blurred and, thus, our distinction between homogenous and heterogeneous catalysts, a comfort-zone classroom concept from the early days of chemistry, needs refinement.[45] One might raise the question, if a complex immobilized on a surface is a homogenous or a heterogeneous catalyst. Furthermore, it cannot be stated unambiguously above which number of atoms small metal clusters or nanoparticles display bulk properties and thus can be considered as heterogeneous catalyst. The size-dependent transition of small clusters towards bulk properties can for instance be traced by the ionization threshold, which is a function of the number of atoms in the cluster[46] and does show an abrupt change. Thus, the catalytic properties of homogenous and heterogeneous catalysts are not expected to be equal, but trends and basic principles are believed to show similarities. Hence, knowledge about the OER mechanism obtained from homogeneous catalysts can act as a starting point for the study of heterogeneous catalysts. With this background experimental insights obtained for heterogeneous catalysts can be judged and parallels can be drawn.

Although a detailed and complete mechanistic picture for heterogeneous benchmark catalysts in acidic media is not available to date, some valuable mechanistic insights have already been published for oxides of Ru, Ir, Pt and Au and will be compared below. The aforementioned catalysts have all been studied by differential electrochemical mass spectroscopy (DEMS) using isotope-labeled electrolytes.[47-52] In these studies, it was demonstrated (possibly with the exception of oxidized Pt) that the metal oxide is likely to participate directly in the OER, at least at the early stages. In other words, a portion of the evolved molecular oxygen originates from the oxide itself. For Pt, however, DEMS studies have remained somewhat contradictory. Willsau et al. found that the oxide layer formed on a Pt electrode does not participate in the OER, since an oxide layer formed in $H_2{}^{18}O$ and then transferred to $H_2{}^{16}O$ for OER yielded only $^{16}O^{16}O$

(m/z=32).[50] Within this study, the authors could verify that an ^{18}O -containing oxide layer remains on the Pt electrode during the transfer.[50] In contrast to that, Churchill et al. found that part of the oxygen evolved on Pt oxide stems from the oxide layer.[51] Hence, at the present state it cannot be unambiguously concluded if the Pt oxide layer directly participates in the OER or not. Arrigo et al. demonstrated in an in-situ near-ambient pressure (NAP) X-ray photoelectron spectroscopy (XPS) study on a sputtered Pt catalyst that up to three different Pt oxides can be formed during the OER.[53] However, even during OER operation at 2 V (against the counter electrode) metallic Pt was detectable by XPS.[53] Based on in-situ NAP-XPS a two-dimensional surface oxide species as well as Pt(II) oxide was identified during the OER.[53] In that study, a Pt(IV) species could only be observed on a Pt foil after prolonged OER at 2.5 V.[53] In contrast to that, Saveleva et al. identified PtO_2 and PtO formation at similar potentials by in-situ NAP-XPS.[54] Whereas the formation of PtO was found to be detrimental for the OER activity, the presence of two-dimensional Pt surface oxide clusters was beneficial and, hence 2D Pt oxide appears to be the active phase for the OER, as illustrated in Figure 6a.[53] However, thick Pt oxide layers, which are likely to be composed of Pt(II) and/or Pt(IV) oxide, are known to display a poor electric conductivity which might be the reason for their detrimental impact on the OER activity.[55] In this context, the observation of Heitbaum et al. that the Pt oxide layer does not participate in the OER appears reasonable, if the term "oxide layer" strictly refers to Pt(II) and/or Pt(IV) oxide and not to the 2D surface oxide. The OER active 2D surface oxide might not be stable enough to sustain the transfer between different electrolytes, which impedes DEMS investigations. Therefore, at the present state neither the *direct coupling* nor the *acid-base mechanism* can be excluded for Pt.

In contrast to that, DEMS results on Au have provided a clearer picture (see Figure 6b). If a gold oxide film is formed in $H_2{}^{18}O$ electrolyte and transferred into $H_2{}^{16}O$ –based electrolyte for OER, initially, only $^{18}O^{18}O$ (m/z=36) was formed.[52] In other words, the initially evolved O_2 stems exclusively from the oxide layer and not from the electrolyte. This result agrees well with the *direct coupling mechanism*. Besides that, surface enhanced Raman spectroscopy (SERS), performed on roughened gold electrodes, revealed the presence of an M-OOH species above 1.4 V_{RHE}, whereas the OER commenced at approximately 2.0 V_{RHE}.[52, 56] Since these events did not emerge at the same potential, the question arises if they are related to each other. Diaz-Morales et al. concluded that the M-OOH species is related to a disordered Au surface oxide which is formed above 1.4 V_{RHE} and then decomposed around 2.0 V_{RHE} under oxygen evolution.[52] The mechanism was hence referred to as “oxide decomposition” mechanism.[52] In line with the nature of an oxide decomposition mechanism, Au dissolution during the OER was found to have the same activation energy as the OER itself, indicating that both processes have a common intermediate.[57] Analyzing the insights obtained for Au in the context of the *direct coupling* versus the *acid-base mechanism*, the reaction mechanism on Au appears more consistent with the former than the latter. At this point it should be noted that M-OOH intermediates may appear in both the *direct coupling* as well as the *acid-base mechanism*.[31]

Hence, these mechanisms cannot be unambiguously distinguished based on the observation of an M-OOH species. However, the combination of DEMS and the SERS results for Au indicates the presence of the *direct coupling mechanism.*

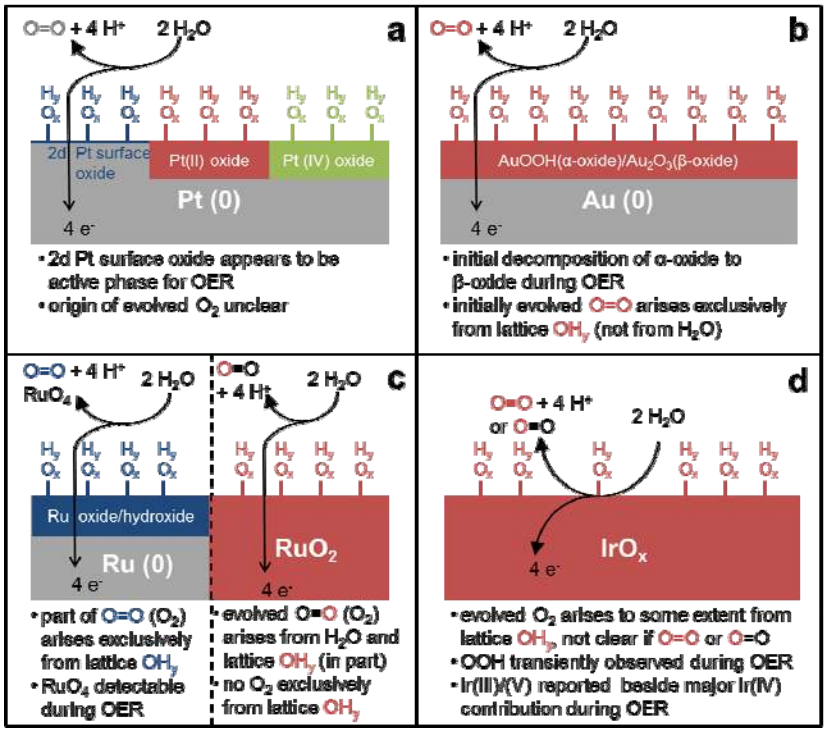

Figure 6: Graphical representation of the experimental in-situ insights into the OER mechanism on Pt (a), Au (b), Ru (electrochemical and thermal oxide) (c) or, respectively, Ir (d) based heterogeneous catalysts. ($0 \leq y \leq 1$, $1 \leq x \leq 2$)

Although Au and Pt have been investigated rather extensively within in-situ OER studies, both materials are, unfortunately, not highly active for the OER. In contrast to that, mechanistic in-situ investigations of highly active Ru oxide catalysts are fairly scarce. Heitbaum et al. demonstrated by DEMS that the Ru oxide layer directly participates in the OER.[47] In case of a Ru oxide layer which was electrochemically prepared in $H_2{}^{18}O$ electrolyte from metallic Ru, the catalytic OER measurement in $H_2{}^{16}O$-based electrolyte revealed the evolution of $^{18}O^{18}O$ (m/z=36),[47] which is indicative for the *direct coupling mechanism*. Furthermore, RuO_4 (m/z= 165) was detected as corrosion product during the OER by DEMS[47] and in-situ reflectance spectroscopy[58]. As reported by Kötz et al., the mechanisms of OER and RuO_4 formation appear to have a common intermediate, since both commence at the same potential.[58] In contrast to that, no RuO_4 formation was reported for thermally prepared RuO_2.[47] Furthermore, a thermally prepared Ru oxide with natural oxygen isotope distribution (mostly ^{16}O) showed no measurable $^{16}O^{16}O$ formation, when it was subjected to OER in $H_2{}^{18}O$ electrolyte.[48] Thus, the *direct coupling mechanism* seems not to be relevant for the OER on thermally prepared RuO_2, suggesting that the

O-O bond formation mechanism is distinctly different on thermally and electrochemically prepared Ru oxide. Oxygen evolution on RuO_2 was also reported to exhibit an interesting electrode potential dependence: At low overpotentials, the molecular oxygen evolved on RuO_2 originated exclusively from water, whereas at higher overpotentials it was formed in parts from the oxide in form of O(oxide)-O(water).[48] Hence, the OER mechanism on thermally prepared crystalline RuO_2 appears not only to differ from that of electrochemical Ru oxide, but it might also be a function of the electrode potential. Due to the apparent sensitivity of the OER mechanism on the preparation and measurement conditions, additional in-situ studies on model catalysts systems are required to shed more light into the complex OER mechanism on Ru oxides.

For thermally prepared IrO_2, a DEMS study with isotope-labeled electrolyte ($H_2{}^{18}O$ enriched) showed that part of the evolved O_2 stemmed from the oxide layer.[49] However, this DEMS study did not address the issue whether O_2 was formed from two oxide lattice-related oxygen atoms or if an oxygen atom from the oxide reacts with water to form O_2. Casalongue et al. observed the presence of an Ir(V) surface species during the OER by in-situ ambient-pressure XPS.[59] However, in the light of new results by Pfeifer et al.[60, 61] this species might actually be an Ir(III) species instead of on Ir(V) species. Minguzzi et al. proposed the presence of an Ir(III) and an Ir(V) species during the OER based on X-ray absorption near-edge structure (XANES) spectroscopy experiments.[62] Furthermore, an Ir oxidation state higher than (IV) was proposed based on in-situ XANES studies of Ir films[63] and Ruthenate-Iridate pyrochlores[64]. However, Ir(V) compounds were commonly not included in the array of reference materials which cast doubt on the edge position based redox state assignment, especially since a shift of the edge position can additionally be induced by a metal-semiconductor transition[65]. Although Ir(V) and Ir(VI) compounds could be isolated within the bulk of crystalline solid state materials,[66] it remains unclear to which extend an Ir species with a charge different to the resting state can build up on the surface of a catalyst with metallic conductivity such as IrO_2. With respect to reactive oxygen surface intermediates, Zhang et al. detected a M-OOH species transiently during oxygen evolution by Fourier transform infrared spectroscopy (FT-IR) on Ir oxide in form of an absorption band at 830 cm^{-1}.[67] However, a SERS study on electrochemically prepared IrO_x revealed no signal around 830 cm^{-1},[68] which indicates that M-OOH species are not present to a large extent during steady state OER operation. Based on these in-situ insights, neither the *acid-base* nor the *direct coupling mechanism* can be conclusively confirmed or dismissed for IrO_x. In this context, more in-depth DEMS investigations might be able to provide additional mechanistic insight.

The chemistry of partly oxidized metal surfaces exhibiting surface and sub-surface oxygen species embedded in a still metallic substrate has been notoriously difficult to detect as frequently documented in chemical catalysis.[69] In the presence of water, the chemical state corresponds to an intermediate stage in the oxidation of a metal surface, resulting in metal acids

$(MO_x(OH)_y)$ n H_2O[70] that may constitute precursors to either dissolution or condensation into a metal acid anhydride $M_xO_y(H_2O)_m$. The general process of transformation of a metal electrode under OER condition requires first and foremost dissolved oxygen atoms in metal (or other local "defects") to allow a hydrophilic bonding of water.[71] In a next step, in order to enable the OER process, the formation of surface oxides occurs concomitant with molecular oxygen gas evolution, followed by hydrolysis to metal acids and finally to metal acid anhydride. It is unlikely that in absence of any thermal activation step dehydrated metal oxide crystals or overlayers will form, unless metal oxide anhydrides are allowed to dehydrate in ambient air conditions over extended timescales.

Reported discrepancies in the detection of intermediates and solid phases by different spectroscopic techniques may be associated with their varying detectability due to weakly scattering surface phases in co-existence with bulk metal or thick deposits of condensates. Radiolytic formation of intermediates or their destruction is an additional source of experimental artifacts and discrepancy. Another challenge is the identification and speciation of aqueous oxidic phases using fingerprint comparisons with bulk oxides that were synthesized by thermal annealing methods. The presence of structural water and residual hydroxyl species in the structure of an "oxide" is inevitable in non-annealed systems. As a result of this, oxide phases may display quite different local and integral electronic properties depending specifically on their electrochemical synthesis protocol. This is why a direct comparison between non-annealed and annealed oxide phases must be done with care, and the speciation using thermal reference compounds may be misleading.

In summary, in-situ studies were performed using many different experimental techniques such as DEMS, XANES, NAP-XPS and, to a minor extent, FT-IR and SERS, although the latter two are underrepresented in this field considering their potential. At first sight it seems disappointing that in the conspectus of this review of past works still no clear picture of a unifying OER mechanism has emerged. The origin of this unsatisfactory situation may be based on insufficient awareness of the fact that an active OER electrode is an electro-catalyst that undergoes dramatic dynamic reorganization[72] during formation and operation. As the active phase requires multi-functionality in terms of adsorption, dissociation and charge carrier mobility, it is likely that only part of these aspects are probed by specific experiments leaving an incomplete picture of the ongoing processes.

Looking ahead, the reviewers suggest that more multi-method and in-situ studies with truly surface sensitive detection methods are conducted. This could clarify the situation and eventually document if a given electrode performs the OER according to different mechanisms under different conditions. The apparent disappointment about the state of knowledge is thus no reason to despair but more a challenge to better respect the dynamical nature of electro-catalytic surfaces.

4. OER Catalysts

This section will address new developments in the field of OER catalyst materials for acidic media with special emphasis on materials that contribute to improve the understanding of the interplay between materials properties and catalytic performance. For a broader overview over OER catalysts in general, their evolution as well as the current state of materials for the application level, the interested reader is referred to other excellent reviews in the field.[5, 7, 73]

4.1. Monometallic Oxides

For the OER on electrochemically oxidized metals a general activity trend has emerged with Ru>Ir>Rh>Pt>Au (see Figure 7).[63, 74-76] This activity trend was established based on the overpotential at a certain geometric current density (5 mA cm^{-2}). Although a comparison based on the intrinsic activity (current normalized to the number of active surface sites, the turn over frequency) would be more precise, it is not feasible at the present state, since the nature of the active center remains elusive. However, since the geometric surface area of polished metals almost matches with the active surface area, the geometric current density constitutes an appropriate measure in the present case. Os was found to be even more active than Ru, but unfortunately it showed a very low stability within the OER.[63] In case of Os only ~5% of the current observable during the OER was related to the OER itself,[63] implying that ~95% of the current was related to corrosion. Hence, in the context of OER, Os can hardly be called a catalyst and is far too unstable for an application on the electrolyzer level. Considering the stability of the other metals, Cherevko et al. found the following trend: Pt>Rh>Ir>Au≥Ru (see Figure 7).[76] Comparing the activity and stability trend, it is apparent that these are not directly anti correlated, although there is a tendency that less active OER catalysts offer a higher stability. However, Au does not follow this trend since it is almost as unstable as the most active catalyst Ru but offers the lowest OER activity within this comparison (see Figure 7). As mentioned in section (3), only in case of Ru and Au indications for a *direct coupling mechanism* were found. Thus, the low stability of Ru and Au might be related to the actual reaction mechanism, as pointed out by Cherevko et al.[76] However, the stability of OER catalysts might be improved by the addition of Pt as stabilizer, since Pt shows a high stability even under elevated temperatures.[77]

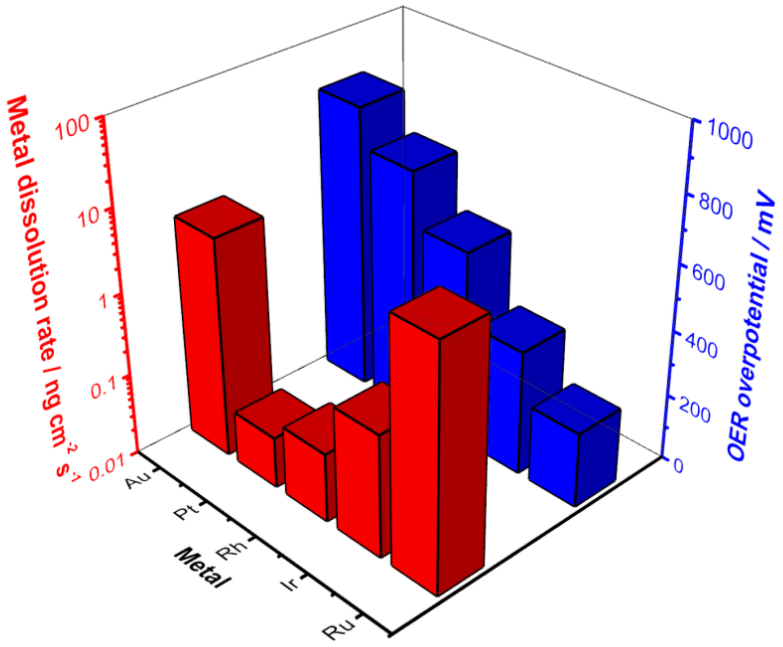

Figure 7: OER performance in form of overpotential and metal dissolution rates at 5 mA cm^{-2} geometric current density of different metal electrodes. The data are obtained from reference [76], were they were obtained by scanning flow cell measurements in conjunction with ICP-MS[78] (electrolyte: 0.1 M H_2SO_4, scan rate: 2 mV s^{-1}, iR corrected).

Apart from the actual metal cation present in an oxide, the synthesis conditions critically determine its OER performance. Thermally prepared oxides were often found to provide a higher stability but a lower activity than electrochemically prepared oxides.[63, 75, 79] Indeed, thermal oxides of Ru and Ir were found to offer a 2-3 orders of magnitude higher stability than their electrochemical analogues.[75] Ir oxide OER catalysts have been prepared in various different ways such as electrochemical[80] or thermal oxidation of metallic Ir[75, 81], physical vapor deposition[82] or the decomposition of suitable precursors[6, 83]. In the latter case, chloride precursors have frequently been applied[81, 84, 85-87] which were often converted, prior to the decomposition, by the Adams fusion method or the Pechini method.[85, 86, 88] If a chloride precursor was used within the thermal decomposition, the resulting oxides were unfortunately found to contain significant amounts of chloride residues.[6] More recently, Ir acetate or Ir acetylacetonate have been used as precursors, which are easy to decompose, either thermally or photochemically, and avoid the chloride contamination problematic.[89-91, 92] Considering Ir oxides, which are prepared by electrochemical oxidation of metallic Ir commonly using cyclic voltammetry, the potential boundaries, number of potential cycles, scan rate, temperature and electrolyte can influence the oxides properties.[93] Additionally, the upper potential boundary was found to impact on the Ir dissolution during oxide formation.[94] The onset of Ir bulk oxide

formation was attributed to the potential range of 0.7-1.1 V_{RHE}, since in this potential range Ir dissolution began.[95] In contrast to electrochemically prepared Ir oxides, the properties of thermally prepared Ir oxides mainly depend on the applied temperature, gas atmosphere and precursor.[85, 90] Oliveira-Sousa et al. demonstrated that the morphology of Ir oxides critically depend on the utilized precursor or, respectively, its pretreatment.[85] Fierro et al. found that Ir oxide prepared by thermal decomposition of H_2IrCl_6 or, respectively, by thermal oxidation of a sputtered metallic Ir film at 500°C resulted in similar voltammograms and surface specific OER activities.[81] This observation indicates that similar Ir oxides were formed and that precursor related differences might not be relevant at high calcination temperatures. However, the OER performance of Ir oxides commonly differs strongly as a function of the preparation conditions. As demonstrated based on thin film Ir oxide model catalysts, the OER performance (in form of the overpotential as well as the stability against dissolution at a certain current density) is a strong function of the calcination temperature, as can be seen in Figure 8.[89, 90, 96] The overpotential is small at the two lowest calcination temperatures and then increases at higher calcination temperatures. In contrast to that, the stability increases with increasing calcination temperature with exception of the film calcined at 350°C. At moderate calcination temperatures (250 and 350°C) an X-ray amorphous, mostly OH terminated, easily reducible Ir oxide phase was formed as major phase.[90] This amorphous Ir oxide phase provided a higher OER activity than the crystalline Ir oxide phase formed at higher calcination temperatures, which is terminated to a larger extent by more strongly bound lattice O species at the surface.[90] The lower stability of the IrO_x(350°C) sample was explained based on the presence of crystalline and amorphous Ir oxide which appeared exclusively for the IrO_x(350°C) sample.[96] An amorphous Ir oxide species with promising OER activity can also be prepared by photochemical decomposition of an Ir acetylacetonate precursor.[92] Pfeifer et al. demonstrated that X-ray amorphous Ir oxide, in contrast to IrO_2, contains a considerable amount of Ir(III) beside Ir(IV) and O 2p hole states which are attributable to a formal O^{1-} species.[60, 61] The O 2p hole states are expected to make the involved O species more electrophilic and, thus, facilitate a nucleophilic attack as described in the *acid-base mechanism*.[60, 97] As explained in section (3), Ir(III) appears to be present to a larger extend under OER conditions and, thus, the increased presence of Ir(III) might additionally be a reason for the higher OER activity of amorphous Ir oxide as it might act as active center for the OER.

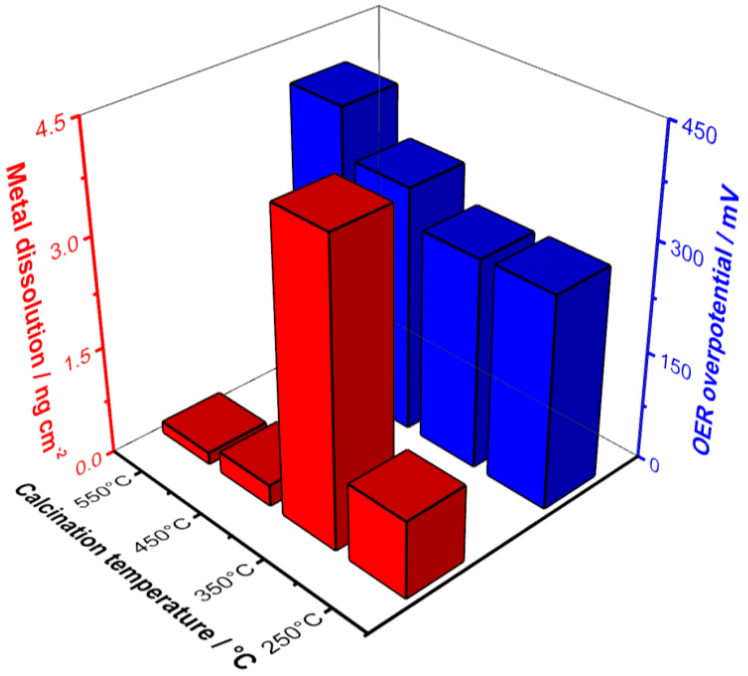

Figure 8: OER performance of thin-film Ir oxide model catalysts in form of overpotential and Ir dissolution as a function of the calcination temperature (constant Ir loading). Overpotentials and integral Ir dissolution during 10 min were measured at a geometric current density of 2 mA cm^{-2}. Overpotentials were taken from reference [90] and Ir dissolution results from reference [96].

Considering the stability and corrosion mechanism of OER catalysts, commonly fewer insights are available than for the OER activity. Generally the focus of OER studies, which is in many cases the catalytic activity, should be extended to the stability, since the catalysts stability is of utmost importance for future device applications. As pointed out by Frydendal et al., assessing the long-term stability in a short-term measurement requires a precise monitoring of catalyst dissolution, for instance by inductively coupled mass spectrometry or quartz crystal microbalance, and cannot be obtained based on short-term purely electrochemical measurements.[98]

For sputtered Ru oxides it was found that the OER activity decreases with increasing deposition temperature while the Ru oxidation state was increased and the surface area was decreased.[99] Both, the higher oxidation state and the lower surface area were thought to cause the observed difference in OER activity.[99] In case of RuO_2, an interesting general synthesis route was found to be the decomposition of RuO_4 as precursor.[100] For mass selected Ru clusters it was demonstrated that crystalline RuO_2, formed by thermal oxidation, is considerably more stable than electrochemical Ru oxide, although it is only slightly less active.[101] These results are in accordance with results obtained by Cherevko et al. for RuO_2 films.[75] Ru particles which were oxidized in an O_2 plasma showed an intermediate behavior.[102] Additionally, the cluster size

impacts the OER activity. For Ru nanoparticles an activity maximum was identified at a particle size of 3-5 nm.[101] Considering RuO_2 crystallites prepared in a sol-gel approach, Macounová et al. demonstrated that the OER activity decreases with increasing crystallite size.[103] Besides particle size effects, the morphology of RuO_2 electrodes on the meso and macro-scale was found to impact the OER activity as it controls the formation and removal of O_2 gas bubbles.[104]

From the above discussion it can be concluded that the OER performance of monometallic Ru and Ir oxides strongly depends on the chemical nature of the actual oxide and its surface properties. Hence, even monometallic oxides of Ru and Ir offer a large optimization potential without the compelling necessity to form mixtures with additional components such as other metal cations. The sensitivity towards the synthesis conditions renders the use of Ru and Ir oxides as reference materials difficult. If Ir or Ru oxide is used as a reference material in an OER study it should be selected and characterized carefully.

For the oxygen reduction reaction (ORR), the reverse reaction of the OER, single-crystal studies revealed the dependence of the ORR activity on the surface structure.[105] But the OER activity also shows a dependence on the surface orientation. Based on strontium ruthenate single-crystal electrodes, Chang et al. showed that the OER activity in an alkaline electrolyte increases in the order (001)<(110)<(111), which is inverse to the stability of these surfaces.[106] This result is supported by findings of Stoerzinger et al. demonstrating that the (100) surface of RuO_2 and IrO_2 is more active in alkaline environment than the more stable (110) surface.[107] Additionally, Danilovic et al. demonstrated in an acidic electrolyte that less defective and, hence, more stable Ru (0001) and Ir (111) single-crystal electrodes are less active than the corresponding polycrystalline electrodes.[63] These result support the idea of a link between activity and stability. Unfortunately, the OER is commonly accompanied by simultaneous metal dissolution.[63, 75, 76, 96, 106, 108] Due to this metal dissolution, the single-crystal surface does not stay intact once the OER commences, as was shown for a strontium ruthenate (001) surface, which was roughened during the OER[109]. Therefore, the activity cannot be correlated unambiguously to the initial surface structure and, thus, the importance of certain surface geometries for the OER activity remains unclear. As recently outlined by Binninger et al., OER with metal dissolution is thermodynamically preferred over OER without metal dissolution, if the electrolyte does not contain ions of those metals present in the catalyst.[108] This explains why a certain amount of metal dissolution is commonly observed during the OER. The inverse relationship between activity and stability observed for different single-crystal surfaces of a certain material can be easily rationalized based on recent in-situ X-ray diffraction studies. Such experiments with Co_3O_4 revealed a reversible structural change of the near surface region during the OER.[110] If it is assumed that the OER can only take place on this structurally modified part of the oxide, it becomes immediately clear that less stable oxide surfaces are beneficial for the activity, since they require a lower driving force (and thus overpotential) for the conversion into the active phase. If the as prepared catalyst is amorphous, its conversion into the actual oxygen-evolving

state requires a lower driving force than the conversion of a highly ordered crystalline oxide. This, in turn, would explain the generally observed higher activity of amorphous catalysts.

4.2. Material concepts beyond monometallic Ru- and Ir oxide catalysts

Ru and Ir oxide catalysts are most frequently optimized through the formation of mixed oxides in order to lower the noble metal content and improve the catalytic activity and/or stability. Partial substitution of the metal cation in an oxide can result in an improved activity due to the alteration of the adsorption strength of reaction intermediates, as outlined by Exner et al.[32]

The most obvious approach to tune the performance of Ru and Ir oxides is to form a mixture of both. This approach has been pursued in many studies during the past decades and it was generally found that the Ru-Ir mixed oxides provide a lower activity but a higher stability than Ru oxide whereas the inverse is true if activity and stability are compared with Ir oxide.[111, 112] Thus, activity and stability can be tuned within the boundaries of the monometallic oxides. Recently, Owe et al. prepared solid solutions of rutile type Ru-Ir mixed oxides by a hydrolysis method.[113] They compared the OER activity of these solid solution mixed oxides with physical mixtures of both components and found similar results as a function of the Ru surface concentration.[113] Hence, no strong synergetic effect appears to be present between Ru and Ir in a solid solution mixed oxide. In contrast to that, Kötz et al. identified a synergistic effect between Ru and Ir for sputtered mixed oxides, since an Ir oxide content of 20% resulted in a reduction of the corrosion rate to approximately 4% of that observed for pure Ru oxide.[112] Similarly, a cooperative effect between Ru and Ir was observed for ruthenate and iridate pyrochlores, $(Na_{0.33}Ce_{0.67})(Ir_{1-x}Ru_x)_2O_7$.[64] In this case, the cooperative effect was identified by in-situ XANES experiments, in which the oxidation state of Ru and Ir at different electrode potentials was found to depend on the composition.[64] The difference with respect to synergetic effects in Ru and Ir mixed oxides indicates that the actual synthesis conditions are at least equally important as for monometallic oxides. Indeed, Danilovic et al. demonstrated that the stability of an Ir-Ru mixed oxide can be varied by surface segregation of Ir without affecting the activity.[114] A mixed oxide with Ir skeleton protective surface layer was ~4 times more stable but similarly as active as a mixed oxide without Ir surface segregation.[114] Thus, the observed differences with respect to the cooperative effect between Ru and Ir might be related to different surface compositions or structures.

Although Ru-Ir mixed oxides are interesting from a fundamental point of view, the optimization of OER activity and stability appears only to be possible within the boundaries of the monometallic oxides. Furthermore, Ru and Ir are both scarce noble metals from the platinum group. A more recent approach for the optimization of Ir and Ru oxides is the formation of mixed oxides with Ni.[19, 103, 115-120] As demonstrated by Macounová et al. Ru-Ni mixed oxides with up to 30% Ni content provide an improved surface specific OER activity over pure Ru oxide.[103] These oxides were composed of a single rutile type phase in which Ni rich clusters or defects

were present and, thus, Ni was not homogenously distributed.[118] As outlined in section 2, the improved OER activity of Ru-Ni mixed oxides was explained based on the formation of a proton-donor-acceptor functionality on the surface caused by Ni ions.[121] However, for stability reasons the optimization of Ir oxides is more interesting. Nong et al. synthesized IrO_x@IrNi core shell nanoparticles which resulted in a substantial lowering of the required Ir amount in an OER catalyst.[116] Furthermore, Nong et al. demonstrated that a high surface area mesoporous antimony doped tin oxide can act as appropriate highly stable support for a good dispersion of this catalyst.[117] For this nano-particulate IrO_x@IrNi catalyst an optimal OER activity was obtained at ~77 at% Ni content, a part of which was leached out electrochemically during the formation of the IrO_x shell.[116] Based on thermally prepared IrNi mixed oxide thin-film model catalysts, Reier et al. showed that the OER activity follows a volcano shaped curve with a maximum in the high Ni range, if normalized to the applied Ir mass or the geometric surface area (see Figure 9a).[115] The surface specific OER activity (current normalized by the surface charge q*) increases with increasing Ni content and shows a plateau at high Ni contents (see Figure 9a).[115] Prior to the OER investigation, part of the Ni was leached out electrochemically from the mixed oxides,[115] which is expected to create Ni vacancies. For the purpose of charge compensation, O species are partially replaced by OH species which results in a change of the oxide surface termination, as illustrated in Figure 9b.[115] The increased number of OH groups, which are expected to be coordinated by a smaller number of metal atoms and, hence, less strongly bound to the oxide backbone, was identified as a likely reason of the improved surface specific OER activity.[115] Additionally, it appears also possible that part of the O^{2-} species are converted into O^{1-} species in order to compensate the negative charge introduced by Ni vacancies, similar to the finding of Pfeifer et al. for amorphous IrO_x[60, 61]. These electrophilic O^{1-} species might be additionally responsible for the improved OER activity, as O^{1-} species are expected to allow for an easier nucleophilic attack of water which is postulated in the *acid-base mechanism*. Based on IrNi mixed oxides, the Ir mass based OER activity could be improved by an impressive factor of ~20.[115]

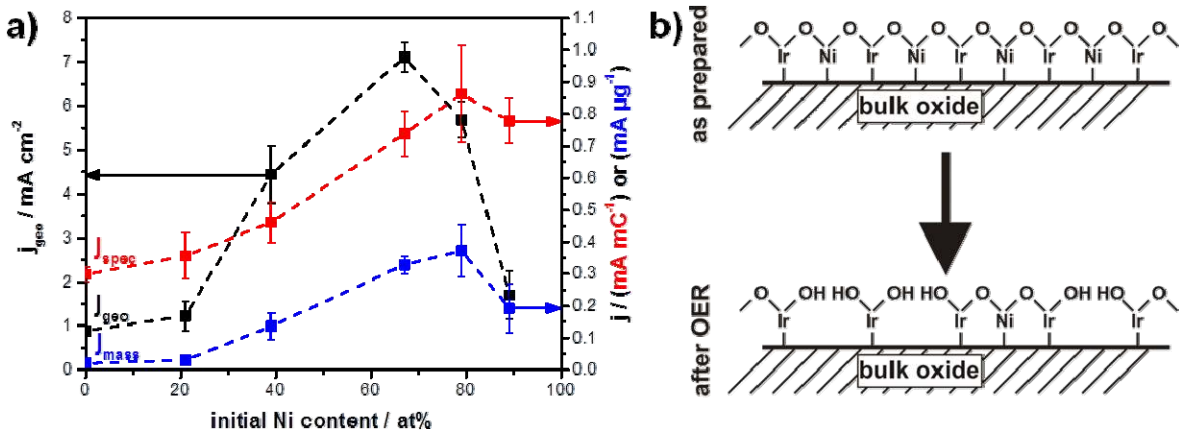

Figure 9: a) OER activity of thermally prepared IrNi mixed oxides films in form of current densities obtained at 1.530 V RHE. The current was normalized with respect to the geometric surface area, the surface charge q (measured between 0.4-1.4 V RHE, with 50 mV s^{-1}) and the applied Ir mass. B) Model for the surface changes of IrNi mixed oxides due to Ni leaching. Reprinted with permission from reference [115]. Copyright (2015) American Chemical Society.*

Beside Ni, many other cations have been used to optimize the catalytic OER performance of Ru and Ir oxide catalysts by the formation of mixed oxides. In case of Ru oxide, mixtures with La[122], Ce[123], Ti[124], Nb[125], Ta,[126], Pb[127], Sn[128], Co[129, 130], Zn[131, 132], Pt[133] and Fe[134] were reported to improve the OER performance. Considering Ir oxides, mixtures with Sn[87, 135], Sb[136], Si[137], Ti[138], Nb[139], Ta[138] or Co[140] were reported and, hence, Ru and Ir oxides were mixed with rather similar components. However, here only selected examples will be discussed in more detail which allow for insights into structure-reactivity relations or provide mechanistic insights. For the other materials the interested reader is referred to a number of excellent reviews.[3, 5, 73, 93] Besides the optimization of Ru and Ir based catalysts, Frydendal et al. introduced a different approach to obtain an acid stable OER catalysts.[141] In this approach an earth-abundant catalyst like MnO_2, which is commonly not stable enough in acidic environment, is stabilized by doping the near surface oxide layers with Ti.[141] Although the OER performance in an acidic electrolyte was poor compared to noble metal catalysts, this appears to be a promising approach, especially if highly active OER catalysts for alkaline environment, such as Ni-Fe oxyhydroxides,[12, 142] can be stabilized in acidic media. Suzuki et al. demonstrated that a cobalt titanium phosphide provided promising OER activity in an acidic environment.[143] Very recently, Patel et al. have reported that fluorine doped $Cu_{1.5}Mn_{1.5}O_4$ is also applicable as OER catalyst in acidic media.[144] As outlined by Binninger et al. the introduction of anions with high oxidation potential can stabilize OER catalysts[108] and, hence, might be one reason for the observed stability of the fluorine doped Cu-Mn mixed oxide under acidic conditions.

Beside Ru-Ni and Ru-Ir mixed oxides, RuZn mixed oxides constitute a very interesting catalyst material.[131, 132] Although the OER activity is only slightly increased due to the addition of Zn, the selectivity for the OER in parallel oxygen and chlorine evolution is strongly increased.[131, 132] The reason for this behavior is related to the materials structure, as reported by Petrykin et al.[132] For the chlorine evolution reaction (ClER), Hansen et al. found in a DFT- based study that the ClER proceeds on RuO_2 via an $Cl(O^c)_2$ intermediate in which O^c refers to O-groups adsorbed on cus sites.[145] Hence, within this model, adjacent cus sites are required to facilitate the ClER on RuO_2.[145] Zn forms very small ilmenite type clusters within the rutile type host structure of RuO_2.[132] These ilmenite clusters decrease the number of adjacent cus O sites.[132] Thus, the observation of a lower ClER activity for a material with decreased number of adjacent cus sites is in agreement with the model for the ClER proposed by Hansen et al. Since the OER activity is not similarly lowered, the adjacent cus oxygen motive appears not to be required for the OER on RuO_2. These experimental observations are in line with the *acid-based reaction mechanism* including the nucleophilic attack of water, since this mechanism is based on a single active center

and, hence, does not involve two active sites at a certain specific distance. A rather similar behavior with respect to the ClER-OER selectivity was observed for Ru-Co mixed oxides.[130]

The previously mentioned optimization concepts for OER catalysts rely on the optimization of synthesis conditions and the substitution of Ru or Ir by other cations. However, anion substitution appears also to be feasible in this context, if the anion bound in the catalyst has a higher oxidation potential than the potentials applied during the OER. Indeed, Kadakia et al. could show that doping IrO_2 with fluorine has a beneficial effect on the OER performance.[146, 147] In particular, the OER activity was improved noticeably by about 19% without affecting the stability of the catalyst.[146] An atomistic explanation for this behavior was given by Velikokhatnyi et al. in which the authors pointed out that the adsorption strength of oxygen surface intermediates on IrO_2 can be increased by fluorine doping.[148] F-ions have a smaller effective charge than O-ions, which leads to a reduced electrostatic repulsion between oxygen surface intermediates and the F-doped IrO_2 surface and, hence, results in a stronger adsorption.[148] The approach of fluorine doping was also extended to mixed oxides like Ir-Sn, Ir-Sn-Nb oxide or Ru-Sn oxide in which the noble metal content is appreciably reduced.[149]

Another approach to optimize the performance of electrocatalysts in general is nano-structuring, which includes the control of size and shape of the catalyst particles. In this context, the control over the particle shape allows to adjust the relative abundance of different crystal facets that are exposed to the electrolyte.[150] Since different facets tend to have different reactivities (see section 4.1), this approach allows for tuning the surface specific catalytic activity. Shape controlled and, similarly, alloy core-shell nanoparticles with a noble metal rich shell have been applied very successfully as concepts for catalyst nano-structuring in the field of ORR, where they yielded in an appreciable activity improvement.[151] Since the OER activity similarly shows a facet dependence (see section 4.1), shape controlled catalysts are of potential interest in the field of OER. Indeed, it was shown that Ir nanodendrites, shape-controlled Ir-Ni nanoparticles and Cu-Ir nanocages show improved OER performances.[120, 152] However, in case of OER catalysts a certain particle shape might be quickly altered within the catalytic process, as the OER is commonly accompanied by metal dissolution (see section 4.1). Beside the shape control, the catalyst can be optimized controlling the size. Small particles provide a large surface area to bulk ratio and, thus, reduce the amount of scarce Ru and Ir catalyst by dispersion. Additionally, a higher surface area to bulk ratio can be obtained when creating mesoporous catalyst films[91, 153], aerogels[154] or nanowire networks[155] besides others.

4.3. Support materials for PEM electrolyzer anode catalysts

Nano-scaled catalysts, shape-controlled or not, can only unfold their full potential, if they are dispersed on an appropriate support material. This support material ideally combines a high electrical conductivity and a high surface area with excellent corrosion stability under the highly corrosive acidic OER reaction conditions. In the context of electrocatalytic applications, carbon-

based support materials such as carbon black, nanotubes, nanofibers; mesoporous carbon or boron doped diamond are widely used, since they commonly provide a high electrical conductivity and a high surface area.[156] Unfortunately, carbon based support materials show stability deficiencies due to corrosion even under potentials present at fuel cell cathodes especially during start-up and shutdown.[157, 158] Commonly, 0.207 V is considered as standard potential for the oxidation of carbon to CO_2 and, hence, carbon based materials are thermodynamically unstable under fuel cell cathode potentials.[156] Since the electrode potentials at PEM electrolyzer anodes are much higher than those of fuel cell cathodes, the driving force for carbon corrosion is even higher in this case. Hence, carbon based materials appear not to be appropriate as support materials for PEM electrolyzers, although a higher degree of graphitization lowers the corrosion problem[157]. The development of doped nanostructured carbon forms based upon nanotubes, graphene and diamond-like carbon shows promising stability in ORR applications.[159] This trend may be carried further to OER conditions, in particular if the issue of initial oxidation of the support followed by the formation of a passive structure can be exploited to anchor the active metal only after initial passivation.

As alternatives support materials Sn-based, In-based, W-based and Ti-based electrically conductive oxides are frequently considered.[156, 160, 161, 162] In case of Ti based oxides, a sufficient electrical conductivity can be ensured by utilization of substochiometric oxides (Ti_nO_{2n-1}, $4 \leq n \leq 10$)[163] or by cation-doping of TiO_2 for instance with Nb[164, 165]. The substochiometric Ti oxide supports offer comparably high electrical conductivities of ~25-1000 S cm^{-1},[163] but provide rather small BET surface areas in the order of only a few $m^2\ g^{-1}$.[156] Furthermore, substochiometric Ti oxide supports were found to degrade under OER conditions losing their high conductivity due to oxidation to less conductive Ti oxides.[166] A promising alternative Ti oxide based support is Nb doped TiO_2 (NTO), since it can be synthesized with a comparably large BET surface area of 136 g m^{-2} [167] and shows a higher stability under OER operation than substochiometric Ti oxide supports[166]. However, mesoporous NTO showed a rather low electrical conductivity of 10^{-6}-10^{-5} S cm^{-1} which could be increased to 0.25 S cm^{-1} by heat treatment, whereas NTO films prepared by atomic layer deposition or pulsed laser deposition showed conductivities of 714 or ~5000 S cm^{-1}, respectively.[164, 168] Hence, some optimization potential remains in case of mesoporous NTO. Beside Ti based oxides, SnO_2 based materials are frequently considered as support for electrocatalysts.[117, 156, 161, 169] In case of SnO_2, which is a wide band gap semiconductor,[170] the required electrical conductivity is commonly ensured by doping with Sb or F.[169, 171-173] The Sb as well as the F doped SnO_2 have been synthesized as mesoporous compound or aerogel resulting in rather large BET surface areas in the rage of 100 $m^2\ g^{-1}$ and above.[169, 172, 173] For mesoporous Sb doped SnO_2 (ATO) and F doped SnO_2 (FTO) conductivities in the range of ~ 0.1-7 S cm^{-1} have been reported.[169, 172] Another conductive oxide which can be used as support material for electrocatalysts is Sn doped In oxide (ITO), for which synthesis procedures are reported that result in large surface areas of more than 100 $m^2\ g^{-1}$.[169, 174] The conductivity of mesoporous ITO samples is commonly in the range of 10^{-3}

to 9.5 S cm^{-1}.[174, 175] The values mentioned so far for oxidic support materials are already close to those of Vulcan, a common carbon based support material, which provides a BET surface area of 235 m^2 g^{-1} and a conductivity of 21.6 S cm^{-1}.[169] Hence, current oxidic support materials provide already a decent electrical conductivity and a high surface area although especially a higher electrical conductivity would be desirable for an application in PEM electrolyzers. Furthermore, the stability of oxidic support materials needs to be determined carefully under different operation conditions, since metal dissolution can become problematic for the ionic conductivity of the proton exchange membrane.

Comparing mesoporous ATO, ITO and FTO based on a similar synthesis approach, Oh et al. found that ATO provided the highest BET surface area as well the highest electrical conductivity.[169] Furthermore, mesoporous ATO was demonstrated to be an excellent support for Ir nanodendrites[176] and IrO_x@IrNi core-shell nanoparticles[117] providing a sufficient electrical conductivity and stability. Besides that, the suitability of ATO and ITO was proven on the electrolyzer level.[86, 177] Additionally to the aforementioned oxides, transition metal carbides are considered as potential support materials for electrocatalysts, especially due to expected improvements of the catalysts stability and intrinsic activity.[178] However, the preparation of high surface area transition metal carbides is often considered to be difficult, although advanced synthetic approaches can result in high surface areas as demonstrated for WC.[179]. Furthermore, transition metal carbides tend to be dissolved or oxidized at high electrode potentials,[178] which is a severe drawback for their application as PEM electrolyzer anode catalyst support. Besides the aforementioned oxides and carbides, novel silicone nanofilaments were reported to act as promising support material in water electrolyzers.[180] One additional aspect in the context of support materials is their interaction with the catalytically active phase, which is not well understood up to now. Catalyst-substrate interactions can result in an improved catalytic performance of the active phase[121, 162, 181] but are rarely studied in the field of OER electrocatalysis. The catalytic performance of Pt nanoparticles for methanol oxidation and ORR was successfully tuned using surface functionalized carbon nanotubes[182] or, respectively, ITO[162]. Hence, catalyst-support interactions might be useful as an additional parameter to tune the activity and stability of PEM-compatible OER catalysts.

5. Conclusions and future outlook

Although many different reaction mechanisms have been proposed for the oxygen evolution reaction on heterogeneous catalysts, so far the detailed reaction mechanism in acidic environment has remained elusive which impedes a knowledge-based catalyst design. In contrast, in-situ experimental insights provided a quite detailed OER reaction scheme for homogenous catalysts. Based on the knowledge obtained for homogenous catalysts, experimental in-situ insights for heterogeneous catalysts are evaluated within this review to uncover similarities and differences.

Unfortunately, the OER mechanism on different OER catalysts in acidic environment appears not to be uniform, which certainly impedes mechanistic investigations. Furthermore, the catalysts surface structure seems to change under OER conditions, which hampers mechanistic investigations based on single crystalline electrodes. However, connecting links need to be established between the different reaction mechanisms proposed to generalize the mechanistic picture. For this purpose, more advanced in-situ insights of well-defined materials are required. In this respect, especially DEMS studies as well as surface sensitive in-situ analytical techniques such as NAP-XPS and surface enhanced Raman spectroscopy appear to be powerful.

Even though the OER reaction mechanism has not been completely resolved, catalyst optimization can be performed based on semi-rational structure-activity-stability relations. Interestingly, OER catalyst optimization does not necessarily require mixed oxides systems, since even Ru and Ir oxides alone provide great optimization potential if their chemical properties and surface state are carefully tuned within the synthesis. Nevertheless, the formation of mixed metal oxides can be used to achieve further improvements in OER activity and/or stability while lowering the noble meal content. Considering the mixed oxide systems, those with Ni appear to be of great interest, since the OER activity can be vastly improved which, in turn, reduces the required noble metal content considerably. As a general tendency, the amorphization of the catalyst leads to a higher activity while the stability is lowered, although these do not appear strictly anti-correlated. Furthermore, an increase in the surface hydroxylation as well as the introduction of more electrophilic oxygen species created via defects seem to be beneficial for the OER activity. To further lower the noble metal content, advanced, electrically conductive, high surface area corrosion stable support materials are required to disperse the catalyst sufficiently. In this context often ATO and ITO are applied, which, however, need further improvements to meet the high demands of electrolyzer anode catalysts.

Finally, the question has to be raised, if noble metals, in particular Ir, will be required as basis for an active and stable PEM electrolyzer anode catalyst. Based on the knowledge compiled within the present review, this question has to be affirmed, at least on the medium-term, since at the present state no noble metal free PEM electrolyzer anode catalyst is known that would provide high stability and activity. However, the key to an economically competitive application on the medium-term is a high atom efficiency with respect to the noble metal, which can be achieved improving the intrinsic OER activity as well as the dispersion and dilution of the active phase. Concepts for these approaches have been outlined within this review. However, based on a more in-depth understanding of the structure-activity-stability relationship as well as the reaction mechanism it might, on the long-term, be possible to develop noble metal free PEM electrolyzer anode catalysts.

6. Acknowledgements

Financial support by the German Research Foundation (DFG) through grant STR 596/3-1 and STR 596/4-1under the Priority Program 1613 “Regeneratively formed fuels by water splitting” is gratefully acknowledged. This work received partial funding by the German Federal Ministry of Education and Research (Bundesministerium für Bildung und Forschung, BMBF) under the grant 03SF0531B and 03SF0527A.

7. Bibliography

[1] P. Moriarty, D. Honnery, Int. J. Hydrogen Energy 2007, 32, 1616; D. Anderson, M. Leach, Energy Policy 2004, 32, 1603.
[2] G. W. Crabtree, M. S. Dresselhaus, M. V. Buchanan, Phys. Today 2004, 57, 39.
[3] J. Herranz, J. Durst, E. Fabbri, A. Patru, X. Cheng, A. A. Permyakova, T. J. Schmidt, Nano Energy 2016.
[4] J. A. Turner, Science 1999, 285, 687.
[5] H. Dau, C. Limberg, T. Reier, M. Risch, S. Roggan, P. Strasser, Chemcatchem 2010, 2, 724.
[6] S. Trasatti, Electrochim. Acta 1984, 29, 1503.
[7] M. Carmo, D. L. Fritz, J. Merge, D. Stolten, Int. J. Hydrogen Energy 2013, 38, 4901.
[8] J. D. Holladay, J. Hu, D. L. King, Y. Wang, Catal. Today 2009, 139, 244.
[9] G. Tjarks, J. Mergel, D. Stolten, in *Hydrogen Science and Engineering: Materials, Processes, Systems and Technology*, Vol. 1 (Eds: D. Stolten, B. Emonts), Wiley-VCH, 2016.
[10] A. Albert, A. O. Barnett, M. S. Thomassen, T. J. Schmidt, L. Gubler, ACS Appl. Mater. Interfaces 2015, 7, 22203.
[11] *CRC Handbook of chemistry and physics*, CRC Press/Taylor and Francis, Boca Raton, FL 2010.
[12] L. Trotochaud, J. K. Ranney, K. N. Williams, S. W. Boettcher, J. Am. Chem. Soc. 2012, 134, 17253; L. Trotochaud, S. L. Young, J. K. Ranney, S. W. Boettcher, J. Am. Chem. Soc. 2014, 136, 6744; S. Klaus, Y. Cai, M. W. Louie, L. Trotochaud, A. T. Bell, J. Phys. Chem. C 2015, 119, 7243; S. Klaus, M. W. Louie, L. Trotochaud, A. T. Bell, J. Phys. Chem. C 2015, 119, 18303.
[13] S. Klaus, L. Trotochaud, M. J. Cheng, M. Head-Gordon, A. T. Bell, Chemelectrochem 2016, 3, 66; M. Gorlin, P. Chernev, J. F. de Araujo, T. Reier, S. Dresp, B. Paul, R. Krahnert, H. Dau, P. Strasser, J. Am. Chem. Soc. 2016, 138, 5603; M. X. Chen, Y. Z. Wu, Y. Z. Han, X. H. Lin, J. L. Sun, W. Zhang, R. Cao, ACS Appl. Mater. Inter. 2015, 7, 21852; S. Chen, J. J. Duan, J. R. Ran, S. Z. Qiao, Adv. Sci. 2015, 2; C. C. L. McCrory, S. H. Jung, J. C. Peters, T. F. Jaramillo, J. Am. Chem. Soc. 2013, 135, 16977; J. Park, J. Kim, Y. Yang, D. Yoon, H. Baik, S. Haam, H. Yang, K. Lee, Adv. Sci. 2016, 3; Y. Z. Wu, M. X. Chen, Y. Z. Han, H. X. Luo, X. J. Su, M. T. Zhang, X. H. Lin, J. L. Sun, L. Wang, L. Deng, W. Zhang, R. Cao, Angew. Chem. Int Edit 2015, 54, 4870.
[14] J. Durst, A. Siebel, C. Simon, F. Hasche, J. Herranz, H. A. Gasteiger, Energ. Environ. Sci. 2014, 7, 2255; N. Danilovic, R. Subbaraman, D. Strmcnik, K. C. Chang, A. P. Paulikas, V. R. Stamenkovic, N. M. Markovic, Angew. Chem. Int. Edit. 2012, 51, 12495.
[15] G. M. Mudd, Ore Geol. Rev. 2012, 46, 106.
[16] J. O. Bockris, J. Chem. Phys. 1956, 24, 817.
[17] B. E. Conway, M. Salomon, Electrochim. Acta 1964, 9, 1599; J. O. M. Bockris, in *Modern Aspects of Electrochemistry*, Vol. 1 (Ed: J. O. M. Bockris), Butterswirth, London 1954.

[18] H. Over, Chem. Rev. 2012, 112, 3356.
[19] N. B. Halck, V. Petrykin, P. Krtil, J. Rossmeisl, Phys. Chem. Chem. Phys. 2014, 16, 13682.
[20] I. C. Man, H. Y. Su, F. Calle-Vallejo, H. A. Hansen, J. I. Martinez, N. G. Inoglu, J. Kitchin, T. F. Jaramillo, J. K. Norskov, J. Rossmeisl, Chemcatchem 2011, 3, 1159.
[21] J. Rossmeisl, A. Logadottir, J. K. Norskov, Chem. Phys. 2005, 319, 178.
[22] J. Rossmeisl, Z. W. Qu, H. Zhu, G. J. Kroes, J. K. Norskov, J. Electroanal. Chem. 2007, 607, 83.
[23] P. Castelli, S. Trasatti, F. H. Pollak, W. E. Ogrady, J. Electroanal. Chem. 1986, 210, 189.
[24] A. G. Scheuermann, J. D. Prange, M. Gunji, C. E. D. Chidsey, P. C. McIntyre, Energy Environ. Sci. 2013, 6, 2487.
[25] M. T. M. Koper, J. Solid State Electrochem. 2013, 17, 339.
[26] T. Nakagawa, C. A. Beasley, R. W. Murray, J. Phys. Chem. C 2009, 113, 12958; M. T. M. Koper, Phys. Chem. Chem. Phys. 2013, 15, 1399; L. Giordano, B. H. Han, M. Risch, W. T. Hong, R. R. Rao, K. A. Stoerzinger, Y. Shao-Horn, Catal. Today 2016, 262, 2.
[27] M. T. M. Koper, Chem. Sci. 2013, 4, 2710.
[28] Reprinted from Journal of Electroanalytical Chemistry, 607, J. Rossmeisl, Z.-W. Qu, H. Zhu, G.-J. Kroes, J. K. Nørskov, Electrolysis of water on oxide surfaces, 83-89, Copyright (2007), with permission from Elsevier
[29] Y. H. Fang, Z. P. Liu, J. Am. Chem. Soc. 2010, 132, 18214.
[30] D. Chen, Y. H. Fang, Z. P. Liu, Phys. Chem. Chem. Phys. 2012, 14, 16612.
[31] M. G. Mavros, T. Tsuchimochi, T. Kowalczyk, A. McIsaac, L. P. Wang, T. Van Voorhis, Inorg. Chem. 2014, 53, 6386.
[32] K. S. Exner, J. Anton, T. Jacob, H. Over, Chemelectrochem 2015, 2, 707.
[33] G. Mattioli, P. Giannozzi, A. A. Bonapasta, L. Guidonili, J. Am. Chem. Soc. 2013, 135, 15353.
[34] L. P. Wang, T. Van Voorhis, J. Phys. Chem. Lett. 2011, 2, 2200.
[35] L. P. Wang, Q. Wu, T. Van Voorhis, Inorg. Chem. 2010, 49, 4543; J. J. Concepcion, M. K. Tsai, J. T. Muckerman, T. J. Meyer, J. Am. Chem. Soc. 2010, 132, 1545.
[36] D. E. Polyansky, J. T. Muckerman, J. Rochford, R. F. Zong, R. P. Thummel, E. Fujita, J. Am. Chem. Soc. 2011, 133, 14649.
[37] J. K. Hurst, J. L. Cape, A. E. Clark, S. Das, C. Y. Qin, Inorg. Chem. 2008, 47, 1753.
[38] R. Cao, W. Z. Lai, P. W. Du, Energ. Environ. Sci. 2012, 5, 8134.
[39] D. J. Wasylenko, C. Ganesamoorthy, B. D. Koivisto, M. A. Henderson, C. P. Berlinguette, Inorg. Chem. 2010, 49, 2202.
[40] Y. Pushkar, D. Moonshiram, V. Purohit, L. F. Yan, I. Alperovich, J. Am. Chem. Soc. 2014, 136, 11938.
[41] Z. F. Chen, J. J. Concepcion, T. J. Meyer, Dalton Transactions 2011, 40, 3789.
[42] Z. F. Chen, J. J. Concepcion, X. Q. Hu, W. T. Yang, P. G. Hoertz, T. J. Meyer, P. Natl. Acad. Sci. USA 2010, 107, 7225.

[43] D. Moonshiram, I. Alperovich, J. J. Concepcion, T. J. Meyer, Y. Pushkar, P. Natl. Acad. Sci. USA 2013, 110, 3765; H. Yamada, J. K. Hurst, J. Am. Chem. Soc. 2000, 122, 5303.
[44] I. Lopez, M. Z. Ertem, S. Maji, J. Benet-Buchholz, A. Keidel, U. Kuhlmann, P. Hildebrandt, C. J. Cramer, V. S. Batista, A. Llobet, Angew. Chem. Int. Ed. 2014, 53, 205.
[45] R. H. Crabtree, Chem. Rev. 2012, 112, 1536.
[46] M. D. Morse, Chem. Rev. 1986, 86, 1049; L. N. Lewis, Chem. Rev. 1993, 93, 2693.
[47] M. Wohlfahrtmehrens, J. Heitbaum, J. Electroanal. Chem. 1987, 237, 251.
[48] K. Macounova, M. Makarova, P. Krtil, Electrochem. Commun. 2009, 11, 1865.
[49] S. Fierro, T. Nagel, H. Baltruschat, C. Comninellis, Electrochem. Commun. 2007, 9, 1969.
[50] J. Willsau, O. Wolter, J. Heitbaum, J. Electroanal. Chem. 1985, 195, 299.
[51] C. R. Churchill, D. B. Hibbert, J. Chem. Soc., Faraday Trans. 1 1982, 78, 2937.
[52] O. Diaz-Morales, F. Calle-Vallejo, C. de Munck, M. T. M. Koper, Chem. Sci. 2013, 4, 2334.
[53] R. Arrigo, M. Havecker, M. E. Schuster, C. Ranjan, E. Stotz, A. Knop-Gericke, R. Schlogl, Angew. Chem. Int. Ed. 2013, 52, 11660.
[54] V. A. Saveleva, V. Papaefthimiou, M. K. Daletou, W. H. Doh, C. Ulhaq-Bouillet, M. Diebold, S. Zafeiratos, E. R. Savinova, J. Phys. Chem. C 2016.
[55] A. Damjanovic, V. I. Birss, D. S. Boudreaux, J. Electrochem. Soc. 1991, 138, 2549.
[56] B. S. Yeo, S. L. Klaus, P. N. Ross, R. A. Mathies, A. T. Bell, Chemphyschem 2010, 11, 1854.
[57] S. Cherevko, A. R. Zeradjanin, A. A. Topalov, G. P. Keeley, K. J. J. Mayrhofer, J. Electrochem. Soc. 2014, 161, H501.
[58] R. Kotz, S. Stucki, D. Scherson, D. M. Kolb, J. Electroanal. Chem. 1984, 172, 211.
[59] H. G. S. Casalongue, M. L. Ng, S. Kaya, D. Friebel, H. Ogasawara, A. Nilsson, Angew. Chem. Int. Ed. 2014, 53, 7169.
[60] V. Pfeifer, T. E. Jones, J. J. Velasco Vélez, C. Massué, M. T. Greiner, R. Arrigo, D. Teschner, F. Girgsdies, M. Scherzer, J. Allan, M. Hashagen, G. Weinberg, S. Piccinin, M. Hävecker, A. Knop-Gericke, R. Schlögl, Phys. Chem. Chem. Phys. 2016, 18, 2292.
[61] V. Pfeifer, T. E. Jones, J. J. V. Velez, C. Massue, R. Arrigo, D. Teschner, F. Girgsdies, M. Scherzer, M. T. Greiner, J. Allan, M. Hashagen, G. Weinberg, S. Piccinin, M. Havecker, A. Knop-Gericke, R. Schlogl, Surf. Interface Anal. 2016, 48, 261.
[62] A. Minguzzi, O. Lugaresi, E. Achilli, C. Locatelli, A. Vertova, P. Ghigna, S. Rondinini, Chem. Sci. 2014, 5, 3591.
[63] N. Danilovic, R. Subbaraman, K. C. Chang, S. H. Chang, Y. J. J. Kang, J. Snyder, A. P. Paulikas, D. Strmcnik, Y. T. Kim, D. Myers, V. R. Stamenkovic, N. M. Markovic, J. Phys. Chem. Lett. 2014, 5, 2474.
[64] K. Sardar, E. Petrucco, C. I. Hiley, J. D. B. Sharman, P. P. Wells, A. E. Russell, R. J. Kashtiban, J. Sloan, R. I. Walton, Angew. Chem. Int. Ed. 2014, 53, 10960.

[65] Y. Soldo, J. L. Hazemann, D. Aberdam, M. Inui, K. Tamura, D. Raoux, E. Pernot, J. F. Jal, J. Dupuy-Philon, Phys. Rev. B 1998, 57, 258.
[66] D. Y. Jung, G. Demazeau, J. H. Choy, High Pressure Res. 1996, 15, 121; G. Demazeau, D. Y. Jung, A. Largeteau, C. Cros, J. H. Choy, J. Alloy Compd. 1997, 262, 191.
[67] N. Sivasankar, W. W. Weare, H. Frei, J. Am. Chem. Soc. 2011, 133, 12976.
[68] S. Z. Zou, H. Y. H. Chan, C. T. Williams, M. J. Weaver, Langmuir 2000, 16, 754.
[69] R. Blume, M. Havecker, S. Zafeiratos, D. Teschner, E. Vass, P. Schnorch, A. Knop-Gericke, R. Schlogl, S. Lizzit, P. Dudin, A. Barinov, M. Kiskinova, Phys. Chem. Chem. Phys. 2007, 9, 3648.
[70] M. Henry, J. P. Jolivet, J. Livage, Struct. Bond. 1992, 77, 153.
[71] A. Teliska, W. E. O'Grady, D. E. Ramaker, J. Phys. Chem. B 2005, 109, 8076.
[72] R. Schlögl, Angew. Chem. Int. Edit. 2015, 54, 3465.
[73] I. Katsounaros, S. Cherevko, A. R. Zeradjanin, K. J. J. Mayrhofer, Angew. Chem. Int. Ed. 2014, 53, 102; E. Antolini, ACS Catal. 2014, 4, 1426.
[74] T. Reier, M. Oezaslan, P. Strasser, ACS Catal. 2012, 2, 1765.
[75] S. Cherevko, S. Geiger, O. Kasian, N. Kulyk, J. P. Grote, A. Savan, B. R. Shrestha, S. Merzlikin, B. Breitbach, A. Ludwig, K. J. J. Mayrhofer, Catal. Today 2016, 262, 170.
[76] S. Cherevko, A. R. Zeradjanin, A. A. Topalov, N. Kulyk, I. Katsounaros, K. J. J. Mayrhofer, Chemcatchem 2014, 6, 2219.
[77] S. Cherevko, A. A. Topalov, A. R. Zeradjanin, G. P. Keeley, K. J. J. Mayrhofer, Electrocatalysis 2014, 5, 235.
[78] S. O. Klemm, A. A. Topalov, C. A. Laska, K. J. J. Mayrhofer, Electrochem. Commun. 2011, 13, 1533; A. K. Schuppert, A. A. Topalov, I. Katsounaros, S. O. Klemm, K. J. J. Mayrhofer, J. Electrochem. Soc. 2012, 159, F670.
[79] S. Geiger, O. Kasian, B. R. Shrestha, A. Mingers, K. J. J. Mayrhofer, S. Cherevko, J. Electrochem. Soc. 2016, 163, F3132.
[80] B. E. Conway, J. Mozota, Electrochim. Acta 1983, 28, 9; J. Mozota, B. E. Conway, Electrochim. Acta 1983, 28, 1; S. Gottesfeld, S. Srinivasan, J. Electroanal. Chem. 1978, 86, 89.
[81] S. Fierro, A. Kapalka, C. Comninellis, Electrochem. Commun. 2010, 12, 172.
[82] G. Beni, L. M. Schiavone, J. L. Shay, W. C. Dautremontsmith, B. S. Schneider, Nature 1979, 282, 281; R. Kotz, H. J. Lewerenz, P. Bruesch, S. Stucki, J. Electroanal. Chem. 1983, 150, 209.
[83] M. H. Miles, Y. H. Huang, S. Srinivasan, J. Electrochem. Soc. 1978, 125, 1931; Y. Matsumoto, T. Tazawa, N. Muroi, E. I. Sato, J. Electrochem. Soc. 1986, 133, 2257; S. Trasatti, in *Electrochemistry of Novel Materials*, Vol. 3 (Eds: J. Lipkowski, P. N. Ross), Wiley-Interscience, 1994.
[84] L. Ouattara, S. Fierro, O. Frey, M. Koudelka, C. Comninellis, J. Appl. Electrochem. 2009, 39, 1361; C. P. De Pauli, S. Trasatti, J. Electroanal. Chem. 1995, 396, 161; L. A. da Silva, V. A. Alves, M. A. P. da Silva, S. Trasatti, J. F. C. Boodts, Can. J. Chem. 1997, 75, 1483.
[85] A. de Oliveira-sousa, M. A. S. da Silva, S. A. S. Machado, L. A. Avaca, P. de Lima-Neto, Electrochim. Acta 2000, 45, 4467.

[86] V. K. Puthiyapura, S. Pasupathi, H. N. Su, X. T. Liu, B. Pollet, K. Scott, Int. J. Hydrogen Energy 2014, 39, 1905.
[87] C. P. De Pauli, S. Trasatti, J. Electroanal. Chem. 2002, 538, 145.
[88] E. Mayousse, F. Maillard, F. Fouda-Onana, O. Sicardy, N. Guillet, Int. J. Hydrogen Energy 2011, 36, 10474.
[89] T. Reier, I. Weidinger, P. Hildebrandt, R. Kraehnert, P. Strasser, ECS Trans. 2013, 58, 39.
[90] T. Reier, D. Teschner, T. Lunkenbein, A. Bergmann, S. Selve, R. Kraehnert, R. Schlogl, P. Strasser, J. Electrochem. Soc. 2014, 161, F876.
[91] E. Ortel, T. Reier, P. Strasser, R. Kraehnert, Chem. Mater. 2011, 23, 3201; M. Bernicke, E. Ortel, T. Reier, A. Bergmann, J. F. de Araujo, P. Strasser, R. Kraehnert, Chemsuschem 2015, 8, 1908.
[92] R. D. L. Smith, B. Sporinova, R. D. Fagan, S. Trudel, C. P. Berlinguette, Chem. Mater. 2014, 26, 1654.
[93] E. Fabbri, A. Habereder, K. Waltar, R. Kotz, T. J. Schmidt, Catal. Sci. Technol. 2014, 4, 3800.
[94] S. Cherevko, S. Geiger, O. Kasian, A. Mingers, K. J. J. Mayrhofer, J. Electroanal. Chem. 2016, 774, 102.
[95] S. Cherevko, S. Geiger, O. Kasian, A. Mingers, K. J. J. Mayrhofer, J. Electroanal. Chem. 2016, 773, 69.
[96] S. Cherevko, T. Reier, A. R. Zeradjanin, Z. Pawolek, P. Strasser, K. J. J. Mayrhofer, Electrochem. Commun. 2014, 48, 81.
[97] V. Pfeifer, T. Jones, S. Wrabetz, C. Massué, J. J. Velasco Vélez, R. Arrigo, M. Scherzer, S. Piccinin, M. Hävecker, A. Knop-Gericke, R. Schlögl, Chem. Sci. 2016.
[98] R. Frydendal, E. A. Paoli, B. P. Knudsen, B. Wickman, P. Malacrida, I. E. L. Stephens, I. Chorkendorff, Chemelectrochem 2014, 1, 2075.
[99] T. J. Kim, S. A. Park, S. Chang, H. H. Chun, Y. T. Kim, Bull. Korean Chem. Soc. 2015, 36, 1874.
[100] A. Kleiman-Shwarsctein, A. B. Laursen, F. Cavalca, W. Tang, S. Dahl, I. Chorkendorff, Chem. Commun. 2012, 48, 967.
[101] E. A. Paoli, F. Masini, R. Frydendal, D. Deiana, C. Schlaup, M. Malizia, T. W. Hansen, S. Horch, I. E. L. Stephens, I. Chorkendorff, Chem. Sci. 2015, 6, 190.
[102] E. A. Paoli, F. Masini, R. Frydendal, D. Deiana, P. Malacrida, T. W. Hansen, I. Chorkendorff, I. E. L. Stephens, Catal. Today 2016, 262, 57.
[103] K. Macounova, J. Jirkovsky, M. V. Makarova, J. Franc, P. Krtil, J. Solid State Electrochem. 2009, 13, 959.
[104] A. R. Zeradjanin, A. A. Topalov, Q. Van Overmeere, S. Cherevko, X. X. Chen, E. Ventosa, W. Schuhmann, K. J. J. Mayrhofer, RSC Adv. 2014, 4, 9579.
[105] N. M. Markovic, R. R. Adzic, B. D. Cahan, E. B. Yeager, J. Electroanal. Chem. 1994, 377, 249; N. M. Markovic, H. A. Gasteiger, N. Philip, 1996, 100, 6715; N. M. Markovic, H. A. Gasteiger, P. N. Ross, 1995, 99, 3411; J. Perez, H. M. Villullas, E. R. Gonzalez, J. Electroanal. Chem. 1997, 435, 179.
[106] S. H. Chang, N. Danilovic, K. C. Chang, R. Subbaraman, A. P. Paulikas, D. D. Fong, M. J. Highland, P. M. Baldo, V. R. Stamenkovic, J. W. Freeland, J. A. Eastman, N. M. Markovic, Nat. Commun. 2014, 5.

[107] K. A. Stoerzinger, L. Qiao, M. D. Biegalski, Y. Shao-Horn, J. Phys. Chem. Lett. 2014, 5, 1636.
[108] T. Binninger, R. Mohamed, K. Waltar, E. Fabbri, P. Levecque, R. Kotz, T. J. Schmidt, Sci. Rep. 2015, 5.
[109] S. H. Chang, J. G. Connell, N. Danilovic, R. Subbaraman, K. C. Chang, V. R. Stamenkovic, N. M. Markovic, Faraday Discuss. 2014, 176, 125.
[110] A. Bergmann, E. Martinez-Moreno, D. Teschner, P. Chernev, M. Gliech, J. F. de Araujo, T. Reier, H. Dau, P. Strasser, Nat. Commun. 2015, 6; C. W. Tung, Y. Y. Hsu, Y. P. Shen, Y. X. Zheng, T. S. Chan, H. S. Sheu, Y. C. Cheng, H. M. Chen, Nat. Commun. 2015, 6.
[111] R. Kotz, S. Stucki, J. Electrochem. Soc. 1985, 132, 103; H. H. Pham, N. P. Nguyen, C. L. Do, B. T. Le, Adv. Nat. Sci.: Nanosci. Nanotechnol. 2015, 6; N. Mamaca, E. Mayousse, S. Arrii-Clacens, T. W. Napporn, K. Servat, N. Guillet, K. B. Kokoh, Appl. Catal., B 2012, 111, 376; T. Audichon, E. Mayousse, S. Morisset, C. Morais, C. Comminges, T. W. Napporn, K. B. Kokoh, Int. J. Hydrogen Energy 2014, 39, 16785.
[112] R. Kotz, S. Stucki, Electrochim. Acta 1986, 31, 1311.
[113] L. E. Owe, M. Tsypkin, K. S. Wallwork, R. G. Haverkamp, S. Sunde, Electrochim. Acta 2012, 70, 158.
[114] N. Danilovic, R. Subbaraman, K. C. Chang, S. H. Chang, Y. J. Kang, J. Snyder, A. P. Paulikas, D. Strmcnik, Y. T. Kim, D. Myers, V. R. Stamenkovic, N. M. Markovic, Angew. Chem. Int. Ed. 2014, 53, 14016.
[115] T. Reier, Z. Pawolek, S. Cherevko, M. Bruns, T. Jones, D. Teschner, S. Selve, A. Bergmann, H. N. Nong, R. Schlogl, K. J. J. Mayrhofer, P. Strasser, J. Am. Chem. Soc. 2015, 137, 13031.
[116] H. N. Nong, L. Gan, E. Willinger, D. Teschner, P. Strasser, Chem. Sci. 2014, 5, 2955.
[117] H. N. Nong, H. S. Oh, T. Reier, E. Willinger, M. G. Willinger, V. Petkov, D. Teschner, P. Strasser, Angew. Chem. Int. Ed. 2015, 54, 2975.
[118] V. Petrykin, Z. Bastl, J. Franc, K. Macounova, M. Makarova, S. Mukerjee, N. Ramaswamy, I. Spirovova, P. Krtil, J. Phys. Chem. C 2009, 113, 21657.
[119] R. B. Moghaddam, C. Wang, J. B. Sorge, M. J. Brett, S. H. Bergens, Electrochem. Commun. 2015, 60, 109.
[120] J. Lim, S. Yang, C. Kim, C. W. Roh, Y. Kwon, Y. T. Kim, H. Lee, Chem. Commun. 2016, 52, 5641.
[121] R. Frydendal, M. Busch, N. B. Halck, E. A. Paoli, P. Krtil, I. Chorkendorff, J. Rossmeisl, Chemcatchem 2015, 7, 149.
[122] M. Abreu-Sepulveda, P. Trinh, S. Malkhandi, S. R. Narayanan, J. Jorne, D. J. Quesnel, J. A. Postonr, A. Manivannan, Electrochim. Acta 2015, 180, 401.
[123] T. Audichon, S. Morisset, T. W. Napporn, K. B. Kokoh, C. Comminges, C. Morais, Chemelectrochem 2015, 2, 1128.
[124] S. Trasatti, Electrochim. Acta 2000, 45, 2377; M. H. P. Santana, L. A. De Faria, Electrochim. Acta 2006, 51, 3578; J. Aromaa, O. Forsen, Electrochim. Acta 2006, 51, 6104; L. A. Naslund, C. M. Sanchez-Sanchez, A. S. Ingason, J. Backstrom, E. Herrero, J. Rosen, S. Holmin, J. Phys. Chem. C 2013, 117, 6126.

[125] V. K. Puthiyapura, S. Pasupathi, S. Basu, X. Wu, H. N. Su, N. Varagunapandiyan, B. Pollet, K. Scott, Int. J. Hydrogen Energy 2013, 38, 8605.
[126] J. Ribeiro, A. R. de Andrade, J. Electroanal. Chem. 2006, 592, 153; J. Ribeiro, M. S. Moats, A. R. De Andrade, J. Appl. Electrochem. 2008, 38, 767.
[127] M. Musiani, F. Furlanetto, R. Bertoncello, J. Electroanal. Chem. 1999, 465, 160.
[128] J. Gaudet, A. C. Tavares, S. Trasatti, D. Guay, Chem. Mater. 2005, 17, 1570; X. Wu, J. Tayal, S. Basu, K. Scott, Int. J. Hydrogen Energy 2011, 36, 14796.
[129] M. V. Makarova, J. Jirkovsky, M. Klementova, I. Jirka, K. Macounova, P. Krtil, Electrochim. Acta 2008, 53, 2656; L. M. Da Silva, J. F. C. Boodts, L. A. De Faria, Electrochim. Acta 2001, 46, 1369; L. M. Da Silva, J. F. C. Boodts, L. A. DeFaria, Electrochim. Acta 2000, 45, 2719; R. Forgie, G. Bugosh, K. C. Neyerlin, Z. C. Liu, P. Strasser, Electrochem. Solid-State Lett. 2010, 13, D36.
[130] V. Petrykin, K. Macounova, M. Okube, S. Mukerjee, P. Krtil, Catal. Today 2013, 202, 63.
[131] V. Petrykin, K. Macounova, O. A. Shlyakhtin, P. Krtil, Angew. Chem. Int. Ed. 2010, 49, 4813.
[132] V. Petrykin, K. Macounova, J. Franc, O. Shlyakhtin, M. Klementova, S. Mukerjee, P. Krtil, Chem. Mater. 2011, 23, 200.
[133] K. C. Neyerlin, G. Bugosh, R. Forgie, Z. C. Liu, P. Strasser, J. Electrochem. Soc. 2009, 156, B363.
[134] K. Macounova, M. Makarova, J. Franc, J. Jirkovsky, P. Krtil, Electrochem. Solid-State Lett. 2008, 11, F27.
[135] G. Li, H. Yu, X. Wang, D. Yang, Y. Li, Z. Shao, B. Yi, J. Power Sources 2014, 249, 175; K. B. Kokoh, E. Mayousse, T. W. Napporn, K. Servat, N. Guillet, E. Soyez, A. Grosjean, A. Rakotondrainibe, J. Paul-Joseph, Int. J. Hydrogen Energy 2014, 39, 1924.
[136] G. H. Chen, X. M. Chen, P. L. Yue, J. Phys. Chem. B 2002, 106, 4364.
[137] J.-J. Zhang, J.-M. Hu, J.-Q. Zhang, C.-N. Cao, Int. J. Hydrogen Energy 2011, 36, 5218; V. H. Tran, T. Yatabe, T. Matsumoto, H. Nakai, K. Suzuki, T. Enomoto, T. Hibino, K. Kaneko, S. Ogo, Chem. Commun. 2015, 51, 12589.
[138] C. Comninellis, G. P. Vercesi, J. Appl. Electrochem. 1991, 21, 335.
[139] W. Hu, S. L. Chen, Q. H. Xia, Int. J. Hydrogen Energy 2014, 39, 6967.
[140] E. L. Tae, J. Song, A. R. Lee, C. H. Kim, S. Yoon, I. C. Hwang, M. G. Kim, K. B. Yoon, ACS Catal. 2015, 5, 5525; J. L. Corona-Guinto, L. Cardeño-García, D. C. Martínez-Casillas, J. M. Sandoval-Pineda, P. Tamayo-Meza, R. Silva-Casarin, R. G. González-Huerta, Int. J. Hydrogen Energy 2013, 38, 12667.
[141] R. Frydendal, E. A. Paoli, I. Chorkendorff, J. Rossmeisl, I. E. L. Stephens, Adv. Energy Mater. 2015, 5.
[142] J. R. Swierk, S. Klaus, L. Trotochaud, A. T. Bell, T. D. Tilley, J. Phys. Chem. C 2015, 119, 19022; H. Ali-Loytty, M. W. Louie, M. R. Singh, L. Li, H. G. S. Casalongue, H. Ogasawara, E. J. Crumlin, Z. Liu, A. T. Bell, A. Nilsson, D. Friebel, J. Phys. Chem. C 2016, 120, 2247.
[143] N. Suzuki, T. Horie, G. Kitahara, M. Murase, K. Shinozaki, Y. Morimoto, Electrocatal. 2016, 7, 115.
[144] P. P. Patel, M. K. Datta, O. I. Velikokhatnyi, R. Kuruba, K. Damodaran, P. Jampani, B. Gattu, P. M. Shanthi, S. S. Damle, P. N. Kumta, Sci. Rep. 2016, 6.

[145] H. A. Hansen, I. C. Man, F. Studt, F. Abild-Pedersen, T. Bligaard, J. Rossmeisl, Phys. Chem. Chem. Phys. 2010, 12, 283.
[146] K. Kadakia, M. K. Datta, P. H. Jampani, S. K. Park, P. N. Kumta, J. Power Sources 2013, 222, 313.
[147] K. S. Kadakia, P. H. Jampani, O. I. Velikokhatnyi, M. K. Datta, S. K. Park, D. H. Hong, S. J. Chung, P. N. Kumta, J. Power Sources 2014, 269, 855.
[148] O. I. Velikokhatnyi, K. Kadakia, M. K. Datta, P. N. Kumta, J. Phys. Chem. C 2013, 117, 20542.
[149] K. S. Kadakia, P. Jampani, O. I. Velikokhatnyi, M. K. Daita, S. J. Chung, J. A. Poston, A. Manivannan, P. N. Kumta, J. Electrochem. Soc. 2014, 161, F868; K. Kadakia, M. K. Datta, O. I. Velikokhatnyi, P. H. Jampani, P. N. Kumta, Int. J. Hydrogen Energy 2014, 39, 664; K. Kadakia, M. K. Datta, O. I. Velikokhatnyi, P. Jampani, S. K. Park, S. J. Chung, P. N. Kumta, J. Power Sources 2014, 245, 362.
[150] Y. J. Wang, N. N. Zhao, B. Z. Fang, H. Li, X. T. T. Bi, H. J. Wang, Chem. Rev. 2015, 115, 3433; N. Tian, Z. Y. Zhou, S. G. Sun, Y. Ding, Z. L. Wang, Science 2007, 316, 732.
[151] C. H. Cui, L. Gan, M. Heggen, S. Rudi, P. Strasser, Nat. Mater. 2013, 12, 765; L. Gan, C. H. Cui, M. Heggen, F. Dionigi, S. Rudi, P. Strasser, Science 2014, 346, 1502; C. H. Cui, L. Gan, H. H. Li, S. H. Yu, M. Heggen, P. Strasser, Nano Lett. 2012, 12, 5885; R. M. Aran-Ais, F. Dionigi, T. Merzdorf, M. Gocyla, M. Heggen, R. E. Dunin-Borkowski, M. Gliech, J. Solla-Gullon, E. Herrero, J. M. Feliu, P. Strasser, Nano Lett. 2015, 15, 7473; Z. C. Liu, C. F. Yu, I. A. Rusakova, D. X. Huang, P. Strasser, Top. Catal. 2008, 49, 241; Z. C. Liu, S. Koh, C. F. Yu, P. Strasser, J. Electrochem. Soc. 2007, 154, B1192; M. Oezaslan, F. Hasche, P. Strasser, J. Electrochem. Soc. 2012, 159, B394; M. Oezaslan, F. Hasche, P. Strasser, Chem. Mater. 2011, 23, 2159; M. Heggen, M. Oezaslan, L. Houben, P. Strasser, J. Phys. Chem. C 2012, 116, 19073; R. Z. Yang, P. Strasser, M. F. Toney, J. Phys. Chem. C 2011, 115, 9074.
[152] W. H. Lee, H. Kim, Catal. Commun. 2011, 12, 408; C. Wang, Y. M. Sui, G. J. Xiao, X. Y. Yang, Y. J. Wei, G. T. Zou, B. Zou, J. Mater. Chem. A 2015, 3, 19669.
[153] D. Chandra, N. Abe, D. Takama, K. Saito, T. Yui, M. Yagi, Chemsuschem 2015, 8, 795.
[154] W. Liu, A. K. Herrmann, N. C. Bigall, P. Rodriguez, D. Wen, M. Oezaslan, T. J. Schmidt, N. Gaponik, A. Eychmuller, Acc. Chem. Res. 2015, 48, 154.
[155] M. Rauber, I. Alber, S. Muller, R. Neumann, O. Picht, C. Roth, A. Schokel, M. E. Toimil-Molares, W. Ensinger, Nano Lett. 2011, 11, 2304.
[156] E. Antolini, E. R. Gonzalez, Solid State Ionics 2009, 180, 746.
[157] L. Castanheira, W. O. Silva, F. H. B. Lima, A. Crisci, L. Dubau, F. Maillard, ACS Catal. 2015, 5, 2184.
[158] H. Tang, Z. G. Qi, M. Ramani, J. F. Elter, J. Power Sources 2006, 158, 1306.
[159] C. H. Choi, S. H. Park, S. I. Woo, Acs Nano 2012, 6, 7084; L. T. Qu, Y. Liu, J. B. Baek, L. M. Dai, Acs Nano 2010, 4, 1321; K. S. Yoo, B. Miller, R. Kalish, X. Shi, Electrochem. Solid. St. 1999, 2, 233.
[160] H. Chhina, S. Campbell, O. Kesler, J. Power Sources 2006, 161, 893; X. Z. Cui, J. L. Shi, H. R. Chen, L. X. Zhang, L. M. Guo, J. H. Gao, J. B. Li, J. Phys. Chem. B 2008, 112, 12024; R. Ganesan, J. S. Lee, J. Power Sources 2006, 157, 217; T. Ioroi, Z.

Siroma, N. Fujiwara, S. Yamazaki, K. Yasuda, Electrochem. Commun. 2005, 7, 183; K. W. Park, K. S. Seol, Electrochem. Commun. 2007, 9, 2256; Y. Liu, S. Shrestha, W. E. Mustain, ACS Catal. 2012, 2, 456; J. Suffner, S. Kaserer, H. Hahn, C. Roth, F. Ettingshausen, Adv. Energy Mater. 2011, 1, 648.
[161] J. Y. Xu, Q. F. Li, M. K. Hansen, E. Christensen, A. L. T. Garcia, G. Y. Liu, X. D. Wang, N. J. Bjerrum, Int. J. Hydrogen Energy 2012, 37, 18629.
[162] Y. Liu, W. E. Mustain, J. Am. Chem. Soc. 2013, 135, 530.
[163] J. R. Smith, F. C. Walsh, R. L. Clarke, J. Appl. Electrochem. 1998, 28, 1021.
[164] J. P. Niemelä, H. Yamauchi, M. Karppinen, Thin Solid Films 2014, 551, 19; Y. D. Wang, B. M. Smarsly, I. Djerdj, Chem. Mater. 2010, 22, 6624.
[165] X. J. Lu, W. G. Yang, Z. W. Quan, T. Q. Lin, L. G. Bai, L. Wang, F. Q. Huang, Y. S. Zhao, J. Am. Chem. Soc. 2014, 136, 419.
[166] G. Y. Chen, S. R. Bare, T. E. Mallouk, J. Electrochem. Soc. 2002, 149, A1092.
[167] B. L. Garcia, R. Fuentes, J. W. Weidner, Electrochem. Solid St. 2007, 10, B108.
[168] Y. J. Liu, J. M. Szeifert, J. M. Feckl, B. Mandlmeier, J. Rathousky, O. Hayden, D. Fattakhova-Rohlfing, T. Bein, Acs Nano 2010, 4, 5373; Y. Furubayashi, T. Hitosugi, Y. Yamamoto, K. Inaba, G. Kinoda, Y. Hirose, T. Shimada, T. Hasegawa, Appl. Phys. Lett. 2005, 86.
[169] H. S. Oh, H. N. Nong, P. Strasser, Adv. Funct. Mater. 2015, 25, 1074.
[170] J. R. Zhang, L. Gao, Mater. Res. Bull. 2004, 39, 2249.
[171] V. Müller, M. Rasp, G. Stefanic, J. H. Ba, S. Gunther, J. Rathousky, M. Niederberger, D. Fattakhova-Rohlfing, Chem. Mater. 2009, 21, 5229.
[172] A. M. Volosin, S. Sharma, C. Traverse, N. Newman, D. K. Seo, J. Mater. Chem. 2011, 21, 13232.
[173] J. P. C. Baena, A. G. Agrios, ACS Appl. Mater. Inter. 2014, 6, 19127.
[174] T. T. Emons, J. Q. Li, L. F. Nazar, J. Am. Chem. Soc. 2002, 124, 8516.
[175] M. Davis, K. Zhang, S. R. Wang, L. J. Hope-Weeks, J. Mater. Chem. 2012, 22, 20163; Y. J. Liu, G. Stefanic, J. Rathousky, O. Hayden, T. Bein, D. Fattakhova-Rohlfing, Chem. Sci. 2012, 3, 2367.
[176] H. S. Oh, H. N. Nong, T. Reier, M. Gliech, P. Strasser, Chem. Sci. 2015, 6, 3321.
[177] V. K. Puthiyapura, M. Mamlouk, S. Pasupathi, B. G. Pollet, K. Scott, J. Power Sources 2014, 269, 451; X. Wu, K. Scott, Int. J. Hydrogen Energy 2011, 36, 5806.
[178] Y. Liu, T. G. Kelly, J. G. G. Chen, W. E. Mustain, ACS Catal. 2013, 3, 1184.
[179] Y. Yan, L. Zhang, X. Y. Qi, H. Song, J. Y. Wang, H. Zhang, X. Wang, Small 2012, 8, 3350.
[180] G. R. Meseck, E. Fabbri, T. J. Schmidt, S. Seeger, Adv. Mater. Interfaces 2015, 2.
[181] E. Fabbri, M. Nachtegaal, X. Cheng, T. J. Schmidt, Adv. Energy Mater. 2015, 5; J. Melke, B. Peter, A. Habereder, J. Ziegler, C. Fasel, A. Nefedov, H. Sezen, C. Woll, H. Ehrenberg, C. Roth, ACS Appl. Mater. Interfaces 2016, 8, 82; B. S. Yeo, A. T. Bell, J. Am. Chem. Soc. 2011, 133, 5587; B. S. Yeo, A. T. Bell, J. Phys. Chem. C 2012, 116, 8394.
[182] S. Y. Wang, F. Yang, S. P. Jiang, S. L. Chen, X. Wang, Electrochem. Commun. 2010, 12, 1646.